
Advances in Black-Box VI: Normalizing Flows, Importance Weighting, and Optimization

Abhinav Agrawal

College of Information & Computer Sciences,
University of Massachusetts Amherst
aagrawal@cs.umass.edu

Daniel Sheldon

College of Information & Computer Sciences,
University of Massachusetts Amherst,
sheldon@cs.umass.edu

Justin Domke

College of Information & Computer Sciences,
University of Massachusetts Amherst
domke@cs.umass.edu

Abstract

Recent research has seen several advances relevant to black-box VI, but the current state of automatic posterior inference is unclear. One such advance is the use of normalizing flows to define flexible posterior densities for deep latent variable models. Another direction is the integration of Monte-Carlo methods to serve two purposes; first, to obtain tighter variational objectives for optimization, and second, to define enriched variational families through sampling. However, both flows and variational Monte-Carlo methods remain relatively unexplored for black-box VI. Moreover, on a pragmatic front, there are several optimization considerations like step-size scheme, parameter initialization, and choice of gradient estimators, for which there are no clear guidance in the existing literature. In this paper, we postulate that black-box VI is best addressed through a careful combination of numerous algorithmic components. We evaluate components relating to optimization, flows, and Monte-Carlo methods on a benchmark of 30 models from the Stan model library. The combination of these algorithmic components significantly advances the state-of-the-art "out of the box" variational inference.

1 Introduction

We consider the problem of automatic posterior inference. A scientist or expert creates a model $p(z, x)$ for latent variables z and observed variable x . For example, z might be population-level preferences for a political candidate in each district in a country, while x is an observed set of polls. Then, we wish to approximate the posterior $p(z|x)$, i.e., determine what the observed data say about the latent variables under the specified model. The ultimate aim of automatic inference is that a domain expert can create a model and get answers without manually tinkering with inference details.

In practice, one often resorts to approximate inference. Markov chain Monte Carlo (MCMC) methods are widely applicable and are asymptotically exact, but maybe slow. Variational inference (VI) approximates the posterior within a tractable family. This can be much faster but is not asymptotically exact. Recent developments led to "black-box VI" methods that, like MCMC, apply to a broad class of models [27, 13, 2].

However, to date, black-box VI is not widely adopted for posterior inference. Moreover, there have been several advances that are relevant to black-box VI, but have been little evaluated in that context. One such advance is normalizing flows, which define learnable densities through a composition of

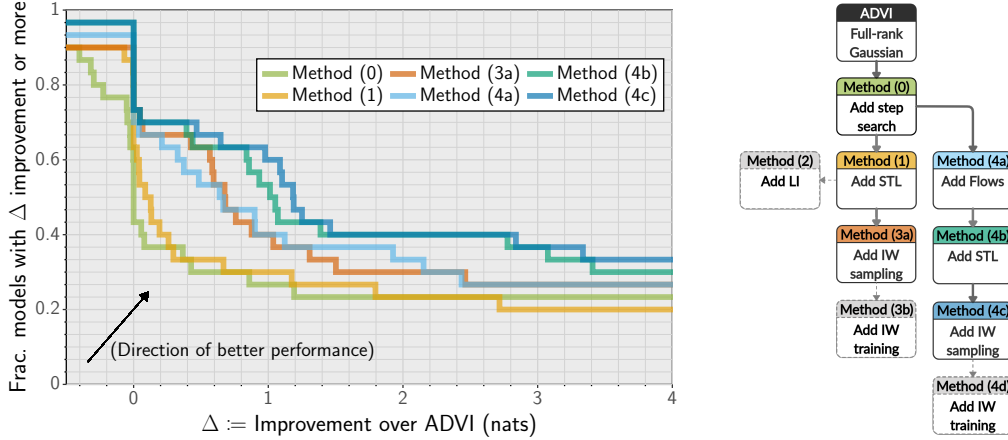


Figure 1: **(Left) Path study:** Empirical complementary-CDF for performance improvement over ADVI. **(Right) Relationship of methods:** Solid lines show modifications that improve performance (included on the left) dotted lines show modifications with unclear benefits (not shown on the left for clarity).

invertible transformations [28, 23]. Surprisingly, normalizing flows have seen almost no investigation for black-box VI; instead, they have been used either to directly learn a density [7, 8, 24, 17] or to bound the likelihood of a deep latent variable model $p_\theta(x) = \int p_\theta(z, x) dz$ [28, 18, 12]. In both cases, there is no mechanistic model and little or no focus on posterior queries.

Another major direction is the development of tighter variational objectives that integrate Monte Carlo techniques such as importance weighting [3, 22, 21]. These were also initially designed to support learning of deep latent variable models. However, further developments have shown that they can also be viewed as enriching the variational family [1, 6, 9, 10]. Still, little is known about the performance of these techniques on real models. Further, importance weighting can be used in two ways. First, importance weighted sampling can be used at inference time to obtain better approximate samples *regardless* of the objective used for optimization. Second, importance weighting can be used during optimization to tighten the objective. There is no evidence in the literature about which approach should be preferred.

It is essential for many users that black-box VI be *fully automatic*. This brings up numerous practical issues, such as initialization, step-size schedules, and the choice of gradient estimator. There have been few attempts to address this [19] and several basic questions remain unanswered: Do recent techniques to enrich variational families such as normalizing flows and variational Monte Carlo methods improve accuracy on mechanistic models? Which of these is more important? Can optimization be made robust enough to work with these techniques “out of the box” on real models?

The basic hypothesis of this paper is that automatic black-box VI can be best achieved through a thoughtful integration of many different algorithmic components. We carefully measure the impact of these components on 30 real models from the Stan model library [32, 33]. Our primary finding is that a combination of techniques to improve optimization robustness and enrich variational families collectively yield remarkable improvements in the accuracy of black-box VI. More concretely, we make the following observations.

- A prior step-size scheme often leads to suboptimal results. Using a comprehensive search over step-sizes is far more reliable (Figure 2).
- When using a Gaussian variational distribution, optimizing with STL gradient estimator [30] that drops the “score term” from the evidence lower-bound (ELBO) gradient is consistently helpful (Figure 3).
- Importance-weighted sampling can be used as a post hoc method to improve the posterior found by *any* inference method. This consistently improves results at minimal cost (Figures 4 and 8)
- Importance-weighted optimization introduces a trade-off between computational complexity and quality. The benefits are not consistent in our experiments (Figures 5 and 9).

- Real-NVP [8] (evaluated for the first time for black-box VI) gives excellent performance. Due to high nonlinearity, one might expect that fully-automatic optimization would be a challenge. However, when combined with our step-size scheme, it consistently delivers strong results with no user-intervention (Figures 6 to 8).
- With normalizing flows, the STL gradient estimator is helpful (Figure 7). However, this uses an inverse transform, which is not efficient with all flows (Section 4.3).
- The doubly-reparameterized estimator [34] consistently improves convergence when applied to optimization with importance weighting (Figure 12 in appendix). However, as above, the overall value of importance-weighted optimization is unclear.

Our final method combines importance sampling, normalizing flows, a highly robust step-size scheme and the variance-reduced estimator STL, to improve the performance by one nat or more on at least 60% of the models when compared to Automatic Differentiation Variational Inference (ADVI) (see performance of Method (4c) in Figure 1). We believe this strategy easily represents the state-of-the-art for fully-automatic black-box VI for posterior inference.

2 Problem Setup

Directly computing the posterior is typically intractable. Variational inference (VI) searches for the closest approximation of $p(z|x)$ within a parameterized family $q_\phi(z)$ by maximizing the evidence lower bound (ELBO) [31]

$$\mathcal{L}(\phi) = \mathbb{E}_{q_\phi(z)} [\log p(z, x) - \log q_\phi(z)] = \log p(x) - \mathbb{KL}[q_\phi(z) \| p(z|x)] \quad (1)$$

Since KL-divergence is non-negative, $\mathcal{L}(\phi)$ lower-bounds $\log p(x)$. Moreover, when p is fixed, optimizing Equation (1) is equivalent to minimizing the KL-divergence between $q_\phi(z)$ and $p(z|x)$.

Exploiting the observations above, there are two basic uses of VI. The first is to *learn* the parameters θ of a model $p_\theta(z, x)$ from examples of x . In this case, VI is used to provide a tractable lower-bound objective over the exact likelihood. This is the basis of variational auto-encoders [16, 29] and their relatives. The second use of VI is to *infer* the posterior $p(z|x)$ of a fixed model. This is the setting of black-box VI [27], the main focus of this paper.

2.1 Rules of engagement

This paper studies many different algorithmic components of black-box VI. Each method is optimized using its own objective to produce an approximate posterior $q_\phi(z)$. During optimization, all methods have the same computational budget, measured as 100 "oracle evaluations" of the $\log p$ per iteration, and are optimized for 30,000 iterations. Then, a *fixed number of 10,000 fresh samples* are drawn from $q_\phi(z)$ to evaluate *either* the ELBO in Equation (1) or the importance-weighted-ELBO in Equation (4). In either case, this gives a lower-bound on $\log p(x)$ (or equivalently an upper-bound on the KL-divergence [9]). Applying importance-weighting can be seen as an *algorithmic component*, not just a "metric" since it gives a different approximation of the posterior [10].

We evaluate each change using a benchmark of 30 models from the Stan Model library [32, 33]. Two inference methods are compared by computing, for each model $i \in \{1, \dots, 30\}$, the difference Δ_i between the lower-bounds produced by the two methods. To remove any possible ambiguity, a standalone description of each method compared is given in Appendix A.

Visualizing results across many models and inference schemes is a challenge. Simple ideas like scatterplots fail because there are many inference schemes and huge differences in $\log p(x)$ across models. Instead, we study results using "empirical complementary CDF plots". The idea is to plot, for each value of Δ , the fraction of values Δ_i that are Δ or higher. This shows how often a given inference method improves on another by a given magnitude Δ .

We start from a simple ADVI baseline model and consider single algorithmic components one by one in Figures 2 to 9. Next, we compare the full "path" of beneficial components to ADVI in Figure 1. Finally, we perform an ablation study removing individual algorithmic components from the final best system in Figure 10. We conduct three independent trials for all of our experiments. For space, the path and ablation study show only a single trial in the main text, with others in the supplement.

3 Optimization in BBVI

Most uses of black-box VI make optimization choices on a model-specific basis. A notable exception to this is the Automatic Differentiation Variational Inference (ADVI) scheme [19], which we use as our baseline. ADVI is integrated into Stan, a state-of-the-art probabilistic programming framework for defining statistical models with latent variables [4]. This makes ADVI one of the most widely available black-box VI algorithms. There are four key ideas: (1) to automatically transform the support of constrained random variables to an unconstrained space (2) to approximate the resulting unconstrained posterior with a Gaussian variational distribution, (3) to estimate the gradient of the ELBO using the reparameterization trick and (4) to do stochastic optimization with a fully-automated step-size procedure.

In all cases, we use the idea of transformation to unconstrained domain unchanged (1). In the rest of this section, we consider modifications to optimization ideas (3,4). In the next section, we consider generalization beyond Gaussians (2).

3.1 ADVI step size search

ADVI uses a novel decreasing step-size scheme based on a base step-size η (we review this in [Appendix E](#)). Authors automate the selection by observing the ELBO values after a fixed small number of iterations for $\eta \in \{0.01, 0.1, 1, 10, 100\}$ and selecting the one that provides the highest final ELBO value, estimated using a batch of fresh samples; we use a batch of fresh 500 samples after 200 iterations. It is not clear to what degree results after a small number of iterations can give a realistic picture of how optimization will look after a large number of iterations. To test this, we propose a straightforward that considers different steps more exhaustively.

3.2 Comprehensive step search

We perform optimization using Adam [15], and we comprehensively search for the Adam step-size η in the range $\frac{0.1}{D} [1, B^{-1}, B^{-2}, B^{-3}, B^{-4}]$, where D is the number of latent dimensions of the model and B is a decay constant; we use $B = 4$. For each step size in this range, we optimize for a fixed number of iterations while keeping the step size constant. The number of iterations is constrained only by the sampling/computational budget of a user; we use 30,000 iterations. Finally, we select the parameters from the step size that led to the best average-objective, averaged over the entire optimization trace. We found this to be a more robust indicator of performance than estimating the final ELBO using a smaller batch of fresh samples (see [Appendix G](#) for discussion).

[Figure 2](#) shows that the comprehensive search provides a significant improvement of 10 nats or more on a small fraction of the models (both schemes in the figure use the closed-form entropy estimator from [Equation \(2\)](#)).

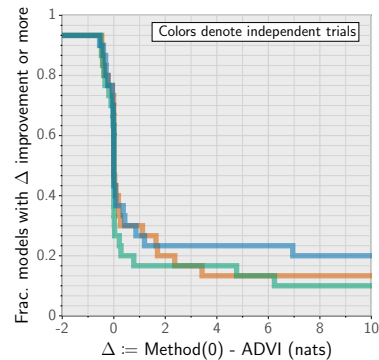


Figure 2: Using comprehensive step-size search provides significant gain of 1 nat on almost 20% of the models (high variability is due to ADVI).

3.3 Gradient Estimation

Most black-box VI methods are based on the reparameterization trick. Suppose that q_ϵ is a fixed distribution and $z_\phi(\epsilon)$ a function such that if $\epsilon \sim q_\epsilon$ then $z_\phi(\epsilon) \sim q_\phi$. Then, if $H(\phi)$ is the entropy of q_ϕ , the gradient of [Equation \(1\)](#) can be written as

$$\nabla_\phi \mathcal{L}(\phi) = \mathbb{E}_{q_\epsilon(\epsilon)} [\nabla_\phi \log p(z_\phi(\epsilon), x)] + \nabla_\phi H(\phi). \quad (2)$$

The gradient can be estimated by drawing a single ϵ (or a minibatch). In some cases (e.g., Gaussians) H is computed in closed form, so the above equation can be used unchanged; this is estimator used in ADVI. Alternatively, ∇H can also be estimated using the reparameterization trick, using either of

$$\nabla_{\phi} H(\phi) = \mathbb{E}_{q_{\epsilon}(\epsilon)} \underbrace{\nabla_{\phi} \log q_{\phi}(z_{\phi}(\epsilon))}_{\text{"Full" estimator}} = \mathbb{E}_{q_{\epsilon}(\epsilon)} \underbrace{(\nabla_{\phi} \log q_{\theta}(z_{\phi}(\epsilon)))_{\theta=\phi}}_{\text{"STL" estimator}}. \quad (3)$$

The second estimator is known as Sticking the landing (STL) gradient [30] and it "holds ϕ constant" under the gradient, which is valid since $\mathbb{E}_{q_{\phi}(z)} \nabla_{\phi} \log q_{\phi}(z) = 0$.

Figure 3 compares the results of the STL estimator to a closed-form entropy. We see that the STL estimator is preferred. We give a more comprehensive comparison of estimators in Figure 11 (supplement).

3.4 Initialization

Initialization can have a major influence on convergence. ADVI initializes to a standard Gaussian. A natural alternative for Gaussian or Elliptical variational distributions is to use Laplace's method to initialize parameters [9, 10]. This method uses black-box optimization to find \hat{z} to maximize $\log p(z, x)$, computes the hessian of $\log p$ at \hat{z} and then sets $q_{\phi}(z)$ to be the Gaussian whose log-density matches the local curvature of $\log p(\hat{z}, x)$. While Laplace's method is natural, it could conceivably be harmful, e.g. by providing an initialization that leads to a worse local optima.

To the best of our knowledge, there are no existing studies of these initialization schemes. Figure 15 (in supplement) uses the previous comprehensive step-size search and compares the results of using Laplace initialization (LI) against not using it. A similar fraction of models are helped and harmed by the change.

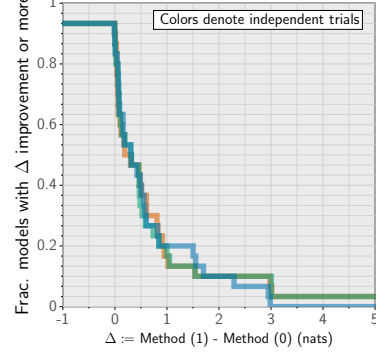


Figure 3: Adding STL to Gaussian VI is consistently helpful across the models and hurts only in minority of cases.

4 Enriched Variational Families

4.1 Monte Carlo Objectives

VI tries to approximate $p(z|x)$ with $q_{\phi}(z)$. If the approximation is inexact, Monte Carlo methods can often improve it. Burda et al. [3] introduced the following "importance-weighted" ELBO (IW-ELBO) to use in place of the conventional ELBO when training a latent-variable model:

$$\mathcal{L}_M(\phi) = \mathbb{E}_{q_{\phi}(z_1) \cdots q_{\phi}(z_M)} \left[\log \frac{1}{M} \sum_{m=1}^M \frac{p(x, z_m)}{q_{\phi}(z_m)} \right] \leq \log p(x). \quad (4)$$

Here, $z_1 \dots z_M$ are iid samples from $q_{\phi}(z)$. This reduces to the standard ELBO when $M = 1$. The IW-ELBO increases with M and approaches $\log p(x)$ asymptotically.

The IW-ELBO is a measure of the accuracy of self-normalized importance sampling on p using q_{ϕ} as a proposal distribution. Define $q_{M,\phi}$ to be the distribution that results from drawing M samples from q_{ϕ} and then selecting one in proportion to the self-normalized importance weights $p(z_m, x)/q_{\phi}(z_m)$. Then, \mathcal{L}_M is a relaxation of the ELBO defined between $q_{M,\phi}$ and the target p [1, 6, 22]. Alternatively, \mathcal{L}_M can be seen as a traditional ELBO between distributions that *augment* $q_{M,\phi}$ and p [9].

For posterior approximation, importance weighting can be applied in two ways.

1. **Importance-weighted sampling.** For *any* distribution, importance-weighting can be applied at test time to improve the quality of the posterior approximation. We know this because $\mathcal{L}_M(\phi) \geq \mathcal{L}(\phi)$ and thus $\mathbb{KL}[q_{M,\phi}(z) \| p(z|x)] \leq \mathbb{KL}[q_{\phi}(z) \| p(z|x)]$ [9]. This should not be

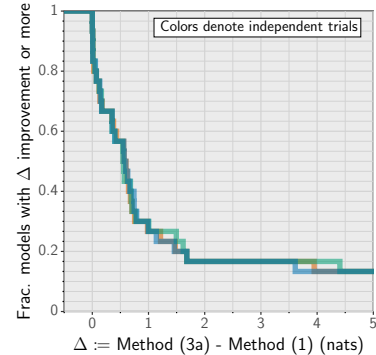


Figure 4: IW-sampling greatly improves the results of Gaussian VI.

seen as a metric for evaluating ϕ . Rather, it is an algorithmic component of inference, since it yields samples that are actually closer to the posterior [10].

2. **Importance-weighted training.** To find the parameters ϕ , one can optimize the IW-ELBO. The idea is that if one intends to perform importance-weighted sampling, this directly optimizes for parameters ϕ that will perform well at this task. That is, optimizing the IW-ELBO implicitly makes $q_{M,\phi}(z)$ close to $p(z|x)$.

Figure 4 shows the results of adding importance-weighted sampling to the previous model, with $M = 10$. This produces a significant benefit of 1 nat or more on 30% of models and never hurts. This also comes at a minimal computational cost since there is no modification of the training procedure. Considerations in importance-weighted training are a bit subtle and discussed next.

4.2 Importance-weighted training

Optimizing Equation (4) requires a gradient estimator. The most obvious estimator is

$$\nabla \mathcal{L}_M(\phi) = \mathbb{E}_{q_\epsilon(\epsilon_1) \cdots q_\epsilon(\epsilon_M)} \sum_{m=1}^M \hat{w}_m \nabla_\phi \log \frac{p(z_\phi(\epsilon_m), x)}{q_\phi(z_\phi(\epsilon_m))}, \quad (5)$$

where $\hat{w}_m = \frac{w_m}{\sum_{l=1}^M w_l}$ for $w_m = \frac{p(x, z_\phi(\epsilon_m))}{q_\phi(z_\phi(\epsilon_m))}$. However, Rainforth et al. [25] point out that the signal-to-noise-ratio of this gradient estimator scales as $1/\sqrt{M}$, suggesting optimization will struggle when M is large. To circumvent this problem, Tucker et al. [34] presented the "doubly reparameterized gradient estimator" (DReG), which does not suffer from the same issue. This is based on the representation of

$$\nabla \mathcal{L}_M(\phi) = \mathbb{E}_{q_\epsilon(\epsilon_1) \cdots q_\epsilon(\epsilon_M)} \sum_{m=1}^M (\hat{w}_m)^2 \nabla_\phi \log \frac{p(z_\phi(\epsilon_m), x)}{q_\theta(z_\phi(\epsilon_m))} \Big|_{\theta=\phi}. \quad (6)$$

Intuitively, the idea is that since θ is ϕ "held constant" under differentiation, the variance is reduced. The difference of the above two estimators is analogous to the difference of the two estimators of the entropy gradient in Equation (3).

We found the DReG out-performed the estimator from Equation (5); using it added 1 nat of improvement to almost 30% of the models (see Figure 12, supplement). However, the benefits are not consistent when compared to IW-sampling alone. Figure 5 shows the performance *decays* on around 20% of models. Thus, when keeping evaluations of $\log p$ fixed at our budget, better performance results from training the regular ELBO with the STL estimator and then using IW-sampling only.

4.3 Normalizing Flows

Normalizing flows construct a flexible class of densities by applying a sequence of invertible transformations to a simple base density. Rezende and Mohamed [28] first introduced normalizing flows in the specific context of approximating distributions for VI; they have since been studied in a much more general context (e.g., for density estimation [8, 17, 12]).

The main idea is to transform a base density $q_\epsilon(\epsilon)$ using a diffeomorphism T_ϕ . The variable $z = T_\phi(\epsilon)$ has the distribution:

$$q_\phi(z) = q_\epsilon(\epsilon) |\det \nabla T_\phi(\epsilon)|^{-1} \quad (7)$$

$$= q_\epsilon(T_\phi^{-1}(z)) |\det \nabla T_\phi^{-1}(z)| \quad (8)$$

Typically, T is chosen as a sequence of transforms, each of which is parameterized by a neural network. These transforms are designed so that the determinant of the Jacobian $|\det \nabla T_\phi(\epsilon)|$ can be computed efficiently.

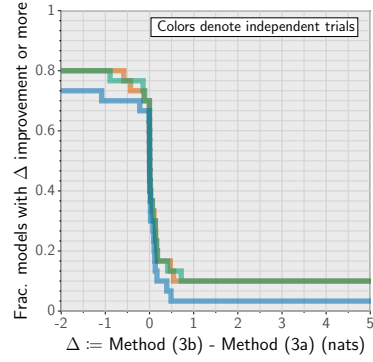


Figure 5: Adding IW-training to IW-sampling offers no clear advantage with Gaussians.

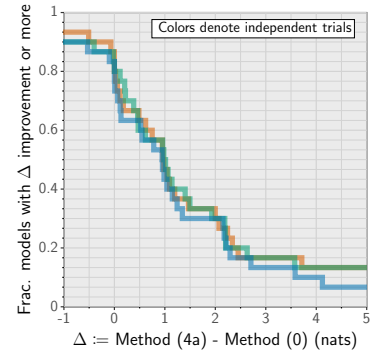


Figure 6: Substituting flows for Gaussians improves half of the models by 1 nat or more.

We use real-NVP—a coupling-based flow [8] with 10 successive transformations, each determined by a fully-connected network with 2 hidden layers each with 32 hidden units (see Appendix F for full details). Figure 6 shows the results of using normalizing flows instead of Gaussians on the benchmark. Since there is no closed-form entropy, these results estimate it using the middle estimator from Equation (3). This yields a significant improvement of 1 nat or more on around half of models.

Depending on the gradient estimator used, the inverse of T_ϕ may or may not be needed. This issue is somewhat subtle. In general, to evaluate the density q_ϕ at an arbitrary point requires computing the inverse T_ϕ^{-1} which may be inefficient [14, 5]. While the ELBO in Equation (1) requires evaluating the density $\log q_\phi$ it is only done on a point sampled from q_ϕ . This means this can be done using only T_ϕ —by first sampling ϵ and then transforming to z there is no need to explicitly compute an inverse. Similarly, if one is to estimate the gradient of the entropy using the “full” estimator (middle equation in Equation (3)), only T_ϕ is needed. However, the estimator that drops the score term (right equation in Equation (3)) is typically lower variance. The natural way to do this is to first sample from q_ϕ , and then, in a second *independent* step, evaluate the sample at parameters $\theta = \phi$ that are held constant under differentiation. In this second step, the sample is treated as an arbitrary point so that derivatives will only flow to the sampling part of the algorithm. This requires the inverse T_ϕ^{-1} .

With real-NVP flows, both the forward and reverse transform are efficient, so the second estimator from Equation (3) can be used. Figure 7 compares the results of substituting this estimator instead. In many cases, the results are much the same. However, in a significant minority of models, the new estimator yields enormous improvements.

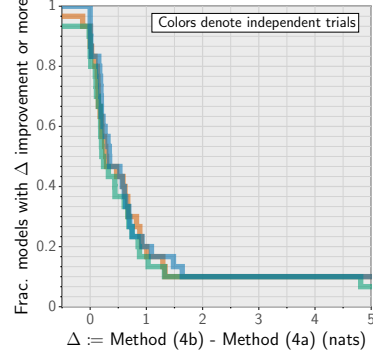


Figure 7: Using the STL estimator for flows (instead of the “full” estimator) is typically helpful and gives huge improvements on a minority of models.

4.4 Importance Weighting with Normalizing Flows

Importance weighting and normalizing flows can be applied together. The ideas in Section 4.1 are not specific to Gaussian densities. In the first experiment, we take the same optimization scheme used above, and apply importance weighted sampling only (with no change to the optimization procedure). As shown in Figure 8, this change never hurts, provides small improvements for most models, and provides large improvements on a minority of models. Since this again comes at a minimal cost (extra work is only needed in the sampling stage) it is very worthwhile.

One can also explicitly optimize the IW-ELBO. Figure 9 demonstrates that adding IW-training provides large benefits on a few models but hurts performance by 1 nat or more for almost 10% of the cases. These observations mirror the effect observed for Gaussians in Figure 5.

We now arrive at our best method: train normalizing flows with a regular ELBO objective using the lower-variance STL gradient and then add importance sampling only during inference. This is easily the go-to black-box VI strategy when we fix a budget for $\log p$ evaluations.

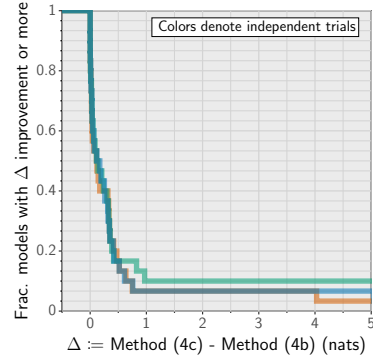


Figure 8: Adding IW-sampling to normalizing flows can significantly improve some of the models and never hurts.

5 Experiments

Using Stan with auto-diff packages: Our experiments are based on a set of models (described in Table 1 in supplement) from the Stan Model library [33, 32]. In order to test our VI variants, we designed a simple interface to use Stan models with VI algorithms implemented in Autograd, a Python automatic differentiation library [20] (refer to Appendix D for more details)

Architectures: For normalizing flow methods, we use real-NVP flow with 10 coupling layers with a fixed base architecture for all models. Complete details are present in [Appendix F](#).

For experiments that use a full-rank Gaussian variational family, we parameterize the mean μ and the Cholesky factor L of the covariance matrix Σ , such that $\Sigma = LL^\top$. Parameters are initialized to a standard normal when Laplace Initialization is not used.

Laplace Initialization: We use SciPy’s BFGS optimize routine to maximize $\log p(z, x)$ over z to get \hat{z} ; we optimize for 2000 iterations (with default settings for other hyper-parameters) [35]. At \hat{z} , we compute the Hessian matrix H using two-point finite differences with $\epsilon = 10^{-6}$. To use LI, we set $\mu = \hat{z}$, and set L such that $LL^\top = (-H)^{-1}$.

Training procedure: To maintain a fair “oracle complexity” in terms of evaluations of $\log p$, each gradient estimate averages over a batch of independent gradient estimates, such that there are always 100 total evaluations of $\log p$ in each iteration. To use [Figure 9](#) as an example, IW-training method averages 10 different copies of the DReG estimator at each iteration ($M = 10$), and IW-sampling method averages 100 different copies of STL estimator (can be viewed as $M = 1$). For all experiments, we use the comprehensive step-size search scheme mentioned in [Section 3](#). Wherever importance weighting is used (sampling or training), $M = 10$

Replicating ADVI: For a fair comparison, we re-implement ADVI optimization in our own framework (refer to [Appendix E](#) for more details). In our preliminary experiments found that the performance matched the PyStan version for the same hyper-parameter settings.

Metric: To compare the performances, we use a fresh batch of 10,000 samples. Again, to maintain a fair “oracle complexity”, we use 10,000 samples irrespective of the M used for importance weighting. To use [Figure 10](#) as an example, when we ablate IW-sampling, we average 10,000 copies of ELBO estimate whereas the “Best model” uses the 1,000 copies of the IW-ELBO estimate ($M=10$).

Results: We provide the complete tables of results with final-metric values from the independent trials in [Appendix J](#) in the supplement.

5.1 Path Study

We summarize the useful algorithmic changes in a path-study by comparing against the common ADVI baseline. [Figure 1](#) presents results from independent trial (see [Figure 13](#) in supplement for full results). Across the trials, we see that with each step in the path performance improves, and the final strategy performs provides significant improvement of 1 nat or more on at least 50% of the models.

5.2 Ablation Study

We analyze the performance of the “best” variational approach by taking away each of it’s components individually. [Figure 10](#) presents the ablation study for an independent trial (see appendix for full results). Across the trials, each component is complementary—they add to the other and the combination performs the best.

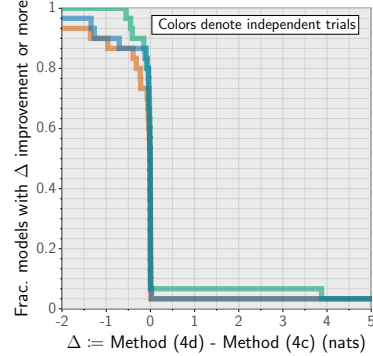


Figure 9: Adding IW-training to IW-sampling offers little advantage with flows.

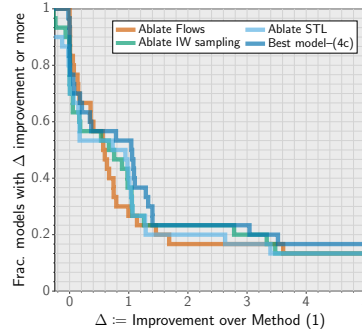


Figure 10: **Ablation Study:** Removing flows has a strong impact; removing STL or IW-sampling has a lesser impact on the performance.

Broader Impact

Mechanistic modeling of natural phenomena is a fundamental quest for modern scientists. In such expeditions, probabilistic models have proved to be a potent tool. However, automatically inferring hidden variables in these models is a challenge to date. Several existing methods either require manual hyperparameter tweaking or perform sub-optimally in exchange for automation.

In this paper, we provide clear empirical evidence that systematically combining recent advances can achieve a robust inference scheme. We successfully redefine the state-of-the-art for “out of the box” approximate inference. Our approach and observations can prove instrumental for researchers in various fields—ecologists, political scientists, social scientists, experimental psychologists, and others.

References

- [1] Philip Bachman and Doina Precup. Training deep generative models: Variations on a theme. In *NIPS Approximate Inference Workshop*, 2015.
- [2] David M Blei, Alp Kucukelbir, and Jon D McAuliffe. Variational inference: A review for statisticians. *Journal of the American statistical Association*, 112(518):859–877, 2017.
- [3] Yuri Burda, Roger Grosse, and Ruslan Salakhutdinov. Importance weighted autoencoders. In *ICLR*, 2016.
- [4] Bob Carpenter, Andrew Gelman, Matthew D Hoffman, Daniel Lee, Ben Goodrich, Michael Betancourt, Marcus Brubaker, Jiqiang Guo, Peter Li, and Allen Riddell. Stan: A probabilistic programming language. *Journal of statistical software*, 76(1), 2017.
- [5] Tian Qi Chen, Jens Behrmann, David K Duvenaud, and Jörn-Henrik Jacobsen. Residual flows for invertible generative modeling. In *NeurIPS*, 2019.
- [6] Chris Cremer, Quaid Morris, and David Duvenaud. Reinterpreting importance-weighted autoencoders. In *ICLR (Workshop)*, 2017.
- [7] Laurent Dinh, David Krueger, and Yoshua Bengio. Nice: Non-linear independent components estimation. In *ICLR (Workshop)*, 2015.
- [8] Laurent Dinh, Jascha Sohl-Dickstein, and Samy Bengio. Density estimation using real NVP. In *ICLR*, 2017.
- [9] Justin Domke and Daniel Sheldon. Importance weighting and variational inference. In *NeurIPS*, 2018.
- [10] Justin Domke and Daniel Sheldon. Divide and couple: Using monte carlo variational objectives for posterior approximation. In *NeurIPS*, 2019.
- [11] John Duchi, Elad Hazan, and Yoram Singer. Adaptive subgradient methods for online learning and stochastic optimization. *Journal of machine learning research*, 12(Jul):2121–2159, 2011.
- [12] Conor Durkan, Artur Bekasov, Iain Murray, and George Papamakarios. Neural spline flows. In *NeurIPS*, 2019.
- [13] Matthew D. Hoffman, David M. Blei, Chong Wang, and John Paisley. Stochastic variational inference. *The Journal of Machine Learning Research*, 14(1):1303–1347, 2013.
- [14] Chin-Wei Huang, David Krueger, Alexandre Lacoste, and Aaron Courville. Neural autoregressive flows. In *ICML*, 2018.
- [15] Diederik P Kingma and Jimmy Ba. Adam: A method for stochastic optimization. In *ICLR*, 2015.
- [16] Diederik P Kingma and Max Welling. Auto-encoding variational bayes. In *ICLR*, 2014.
- [17] Durk P Kingma and Prafulla Dhariwal. Glow: Generative flow with invertible 1x1 convolutions. In *NeurIPS*, 2018.

- [18] Durk P Kingma, Tim Salimans, Rafal Jozefowicz, Xi Chen, Ilya Sutskever, and Max Welling. Improved variational inference with inverse autoregressive flow. In *NeurIPS*, 2016.
- [19] Alp Kucukelbir, Dustin Tran, Rajesh Ranganath, Andrew Gelman, and David M Blei. Automatic differentiation variational inference. *The Journal of Machine Learning Research*, 18(1):430–474, 2017.
- [20] Dougal Maclaurin, David Duvenaud, and Ryan P Adams. Autograd: Effortless gradients in numpy. In *ICML AutoML (Workshop)*, 2015.
- [21] Chris J Maddison, John Lawson, George Tucker, Nicolas Heess, Mohammad Norouzi, Andriy Mnih, Arnaud Doucet, and Yee Teh. Filtering variational objectives. In *NeurIPS*, 2017.
- [22] Christian A Naesseth, Scott W Linderman, Rajesh Ranganath, and David M Blei. Variational sequential monte carlo. In *AISTATS*, 2018.
- [23] George Papamakarios, Eric T. Nalisnick, Danilo Jimenez Rezende, Shakir Mohamed, and Balaji Lakshminarayanan. Normalizing flows for probabilistic modeling and inference. *CoRR*. URL <http://arxiv.org/abs/1912.02762>.
- [24] George Papamakarios, Theo Pavlakou, and Iain Murray. Masked autoregressive flow for density estimation. In *NeurIPS*, 2017.
- [25] Tom Rainforth, Adam R Kosiorek, Tuan Anh Le, Chris J Maddison, Maximilian Igl, Frank Wood, and Yee Whye Teh. Tighter variational bounds are not necessarily better. In *ICML*, 2018.
- [26] Rajesh Ranganath, Chong Wang, Blei David, and Eric Xing. An adaptive learning rate for stochastic variational inference. In *ICML*, 2013.
- [27] Rajesh Ranganath, Sean Gerrish, and David Blei. Black box variational inference. In *Artificial Intelligence and Statistics*, 2014.
- [28] Danilo Jimenez Rezende and Shakir Mohamed. Variational inference with normalizing flows. In *ICML*, 2015.
- [29] Danilo Jimenez Rezende, Shakir Mohamed, and Daan Wierstra. Stochastic backpropagation and approximate inference in deep generative models. In *ICML*, 2014.
- [30] Geoffrey Roeder, Yuhuai Wu, and David K Duvenaud. Sticking the landing: Simple, lower-variance gradient estimators for variational inference. In *NeurIPS*, 2017.
- [31] Lawrence K Saul, Tommi Jaakkola, and Michael I Jordan. Mean field theory for sigmoid belief networks. *Journal of artificial intelligence research*, 4:61–76, 1996.
- [32] Stan Developers. *Example Models*, 2018. URL <https://github.com/stan-dev/example-models>.
- [33] Stan Development Team. *The Stan Core Library, Version 2.18.0.*, 2018. URL <http://mc-stan.org>.
- [34] George Tucker, Dieterich Lawson, Shixiang Gu, and Chris J Maddison. Doubly reparameterized gradient estimators for monte carlo objectives. In *ICLR*, 2019.
- [35] Pauli Virtanen, Ralf Gommers, Travis E. Oliphant, Matt Haberland, Tyler Reddy, David Cournapeau, Evgeni Burovski, Pearu Peterson, Warren Weckesser, Jonathan Bright, Stéfan J. van der Walt, Matthew Brett, Joshua Wilson, K. Jarrod Millman, Nikolay Mayorov, Andrew R. J. Nelson, Eric Jones, Robert Kern, Eric Larson, CJ Carey, İlhan Polat, Yu Feng, Eric W. Moore, Jake VanderPlas, Denis Laxalde, Josef Perktold, Robert Cimrman, Ian Henriksen, E. A. Quintero, Charles R Harris, Anne M. Archibald, Antônio H. Ribeiro, Fabian Pedregosa, Paul van Mulbregt, and SciPy 1.0 Contributors. SciPy 1.0: Fundamental Algorithms for Scientific Computing in Python. *Nature Methods*, 17:261–272, 2020. doi: <https://doi.org/10.1038/s41592-019-0686-2>.

A Full Method Description

ADVI Baseline

Uses a full-rank Gaussian initialized to standard normal and optimizes with closed-form entropy gradient from Equation (2); uses ADVI step-scheme for updates (see Appendix E for more details). Importance-weighted sampling is not used; importance-weighted training is not used (optimized standard ELBO).

Method (0)

Uses a full-rank Gaussian initialized to standard normal and optimizes with closed-form entropy gradient from Equation (2); uses our comprehensive step-size search for updates (see Section 3.2 for more details). Importance-weighted sampling is not used; importance-weighted training is not used.

Method (1)

Uses a full-rank Gaussian initialized to standard normal and optimizes with the STL from Equation (3); uses our comprehensive step-size search for updates. Importance-weighted sampling is not used; importance-weighted training is not used.

Method (2)

Uses a full-rank Gaussian and initializes with LI method from Section 3.4; optimizes with the STL from Equation (3) and uses our comprehensive step-size search for updates. Importance-weighted sampling is not used; importance-weighted training is not used.

Method (3a)

Uses a full-rank Gaussian initialized to standard normal and optimizes with the STL gradient from Equation (3); uses our comprehensive step-size search for updates. Importance-weighted sampling is used with $M = 10$; importance-weighted training is not used.

Method (3b)

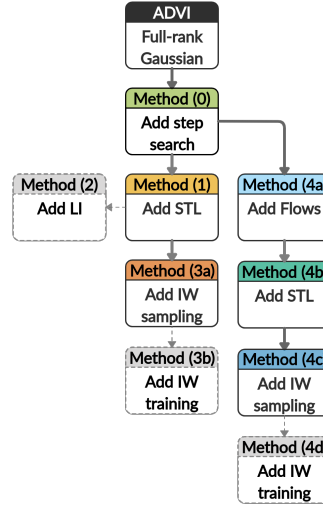
Uses a full-rank Gaussian initialized to standard normal and uses importance-weighted training with $M = 10$; optimizes with the DReG from Equation (6) and uses our comprehensive step-size search for updates. Importance-weighted training is used with $M = 10$ (optimizes IW-ELBO with $M = 10$).

Method (4a)

Uses a real-NVP normalizing flow (see Appendix F for architectural and initialization details) as q_ϕ ; optimizes with the “full” gradient from Equation (3) and uses our comprehensive step-size search for updates. Importance-weighted sampling is not used; importance-weighted training is not used.

Method (4b)

Uses a real-NVP normalizing flow and optimizes with the STL gradient from Equation (3); uses our comprehensive step-size search for updates. Importance-weighted sampling is not used; importance-weighted training is not used.



Method (4c)

Uses a real-NVP normalizing flow and optimizes with the STL gradient from Equation (3); uses our comprehensive step-size search for updates. Importance-weighted sampling is used with $M = 10$; importance-weighted training is not used.

Method (4d)

Uses a real-NVP normalizing flow and uses importance-weighted training with $M = 10$; optimizes with the DReG gradient from Equation (6) and uses our comprehensive step-size search for updates. Importance-weighted training is used with $M = 10$.

B Extended results

B.1 Different gradient for Gaussian VI

There are three choices of gradients for the Gaussian family. First, as Gaussians have a closed-form entropy, we can use the gradient from Equation (2); this is the gradient that ADVI uses. Second, we can alternatively use the middle gradient from Equation (3). Third, we can drop the score-function term and use the STL estimator (third term in Equation (3)). In Figure 11, the first panel compares the performance of using STL against the ADVI implementation (ADVI step-scheme and gradient). In the second panel, we compare the performance with the closed-form estimator optimized using our comprehensive step-search. Finally, we compare against the middle gradient in Equation (3). In all the alternatives, STL rarely hurts and adds significant value to several models.

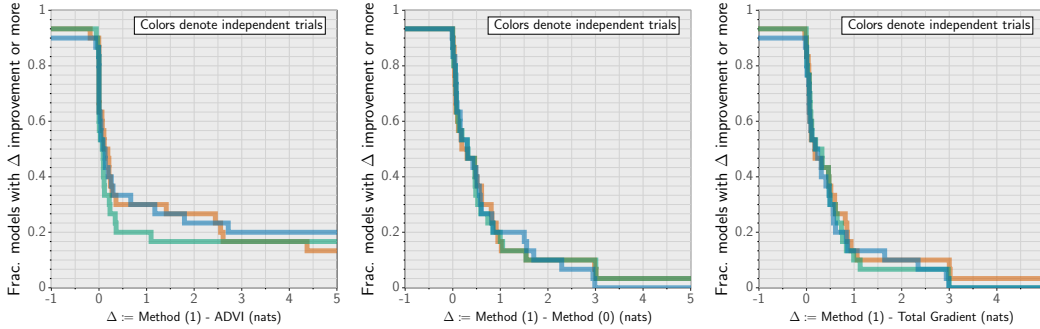


Figure 11: (a) STL against ADVI; STL improves the performance by 1 nat or more on almost 30% of the models. (b) Next, we replace the ADVI step-size scheme with our comprehensive step search. STL improves the performance on 20% of the models by 1 nat or more. (c) We also compare against the middle gradient from Equation (3) and find that STL provides an improvement of 1 nat or more on almost 10% of the models. In all the alternatives, STL rarely hurts.

B.2 IW-training with DReG

We compare IW-training with and without DReG estimator on different possibilities and find that it consistently improved the performance. In Figure 12, we first compare the performance with the standard IW-ELBO gradient for Gaussian families. In the second comparison, we add Laplace Initialization to both methods, IW-ELBO gradient and DReG gradient. In the final comparison, we compare DReG with regular IW-ELBO gradient for normalizing flows. Across all comparisons, DReG improves the performance and rarely hurts.

B.3 Path Study - full results

We conduct a path-study to accumulate all the useful combinations of our analysis. Figure 13 presents the study for three independent trials. The high variation is due to the ADVI; on 10 models out of 30, ADVI diverges in at-least one trial for our implementation. If an optimization diverges, we set the improvement as zero, that is, we count the model in favor of the baseline (see Table 2 for values).

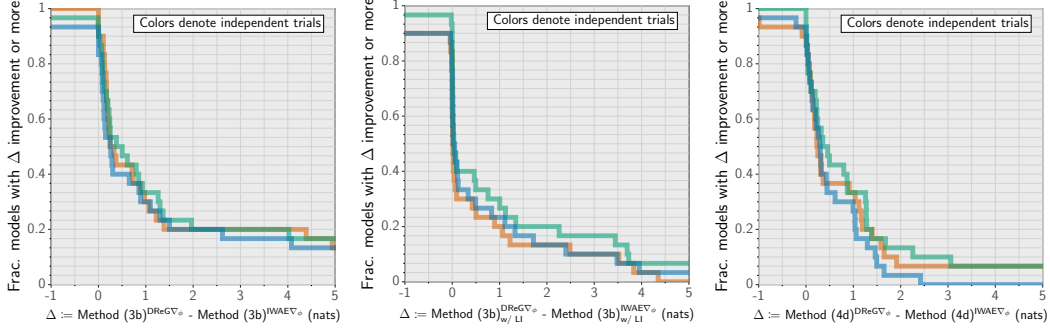


Figure 12: (a) DReG improves the performance significantly by 1 nat on almost 30% of the models for Gaussians when initialized with standard normal (b) On adding LI to the previous model, DReG adds 1 nat to around 20% of the models (c) Adding DReG to IW-training of flows also helps. We observe significant improvement of 1 nat or more for almost 30% of the models

B.4 Ablation Study - full results

We conduct an ablation-study to analyze each component of the best performing method. Figure 13 presents the study for three independent trials.

B.5 Laplace Initialization

Figure 15 compares the results of using Laplace initialization (LI) against not using it (we omitted this comparison from the main text for brevity). While there is a significant improvement on a minority of models, similar fraction observe a significant decay.

C General comment on trade-offs

We note that a trade-off exists between the improvement in performance and the computational complexity we are prepared to entertain (with the increase in the availability of computational resource, we believe this will increasingly tilt in favor of performance). Using a comprehensive step-search scheme is often done in parallel. However, we do stress that a trade-off exist between spending a higher fixed computational cost vs manually tuning the performance. Adding Laplace Initialization requires one to solve a maximization problem beforehand (this is often inexpensive). Adding normalizing flows increase the complexity in terms of both memory and computational time. Adding Importance Weighting with a fixed “Oracle budget” for querying $\log p$ may seem to be relatively inexpensive while training, however, the posterior inference scales linearly in M . Finally, DReG or STL calculation comes at an additional cost for normalizing flows due to a second pass of T_ϕ^{-1} (see Section 4.3 for details).

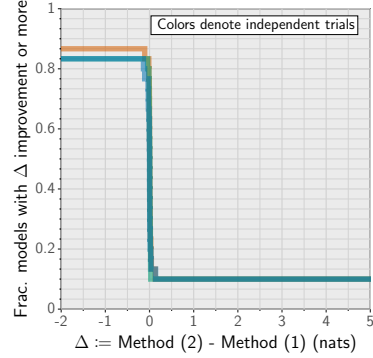


Figure 15: Adding LI to Gaussian VI is neither consistently helpful nor consistently harmful.

D Interfacing using auto-diff packages

To interface with Stan models, we must define a new “primitive” function in Autograd that corresponds to $\log p(x, z)$ as a function of z . In addition, this also requires computing $\log p(x, z)$ itself as well as the gradient-vector product $a^\top \nabla_z \log p(z, x)$ for any vector a . This is easily done since PyStan interface allows access to $\log p(z, x)$ and the gradient $\nabla_z \log p(z, x)$ for any model defined in Stan. This approach has the disadvantage that high-order gradients are not possible. Similar strategies could be used with other automatic differentiation packages.

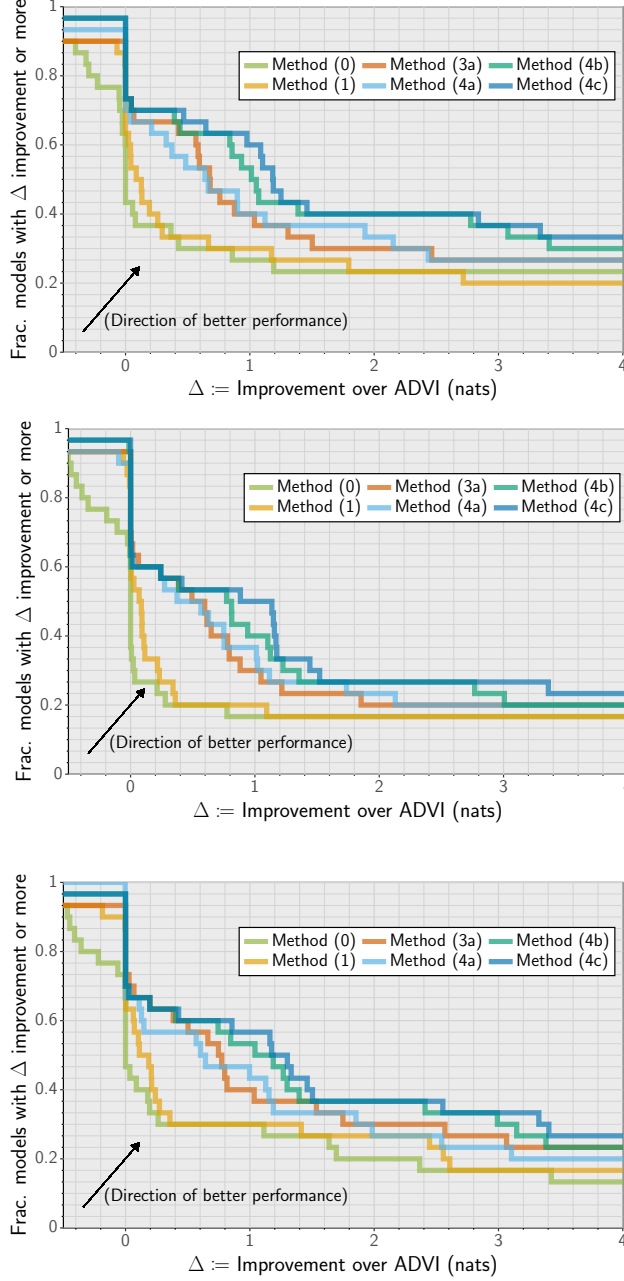


Figure 13: Across the trials: Method (1) that uses STL gradient improves over ADVI by 1 nat or more for at least 20% of the models. Method (3a) adds the IW-sampling to (1) and improves by a nat or more on at least 30% of the models. Method (4a) uses flow with the naive gradient estimator and achieves performance similar to (3a). Method (4b) adds the STL gradient to (4a) and improves on at least 40% of the models by 1 nat or more. Method (4c) adds IW-sampling to (4b) and improves by 1 nat on a minimum of 50% of the models. All our methods use comprehensive step-search and use $M = 10$ wherever IW-sampling is applied.

E ADVI

Step-size scheme ADVI uses a novel step-size sequence inspired by adaptive step-size gradient schemes [11, 26, 15]. The update at iteration i is

$$\phi^{(i+1)} = \phi^{(i)} - \rho^{(i)} \odot g^{(i)}, \quad (9)$$

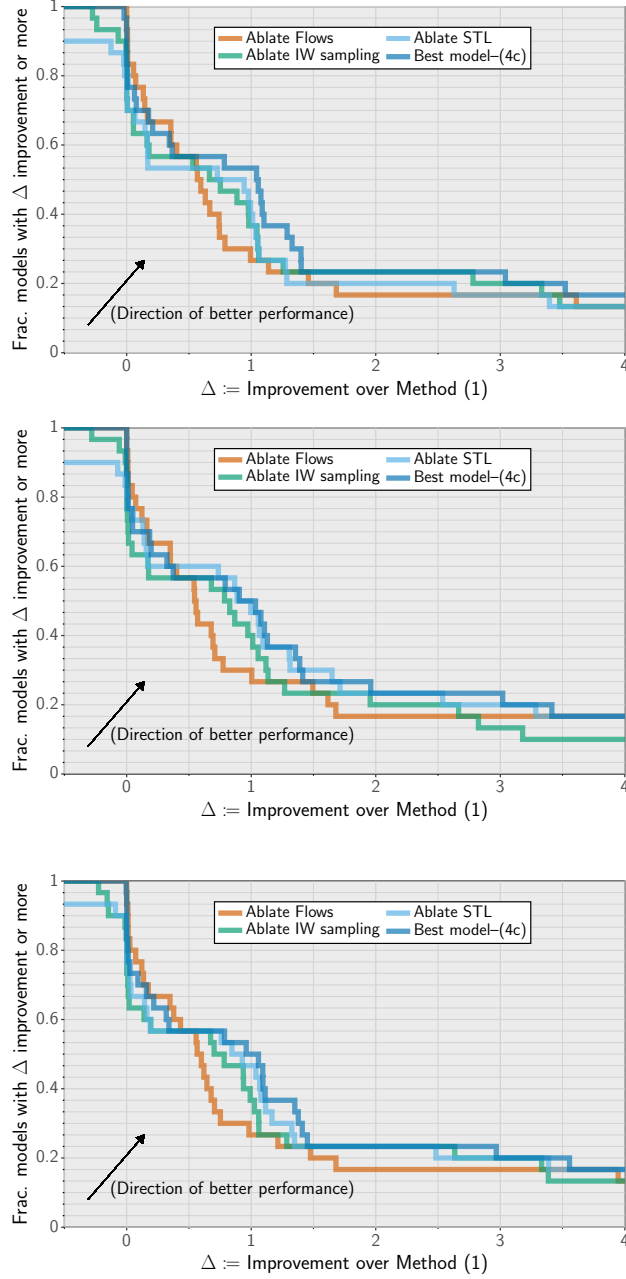


Figure 14: Across the trials: Ablating STL observes the least decay in performance while ablating flows causes the most decrease. The effect of ablating IW-sampling lies somewhere in the middle of these two. All approaches are trained with comprehensive step-search and use $M=10$ wherever importance weighted sampling is used.

where $g^{(i)}$ is the stochastic gradient in the i -th iteration, $\rho^{(i)}$ is a vector of step-sizes (one per coordinate of ϕ) and \odot denotes elementwise multiplication. To determine the stepsizes, a vector $s^{(i)}$ is initialized to $s^{(1)} = (g^{(1)})^2$ and maintained recursively as

$$s^{(i)} = \alpha(g^{(i)})^2 + (1 - \alpha)s^{(i-1)}, . \quad (10)$$

Then, the stepsizes are chosen as

$$\rho^{(i)} = \frac{\eta}{i^{1/2+\epsilon} \times (\tau + \sqrt{s^{(i)}})}, \quad (11)$$

where the square root and division are element-wise. Here $\eta > 0$ is the scale of the step-size, $i^{1/2+\epsilon}$ decays the step over time, and the $s^{(i)}$ adapts the curvature of the ELBO. $\tau = 1$ and $\epsilon = 10^{-16}$ are stabilizing constants.

Implementation details ADVI step-scheme search for η from Equation (11) over the range $\{0.01, 0.1, 1, 10, 100\}$ to best adapt to the size of the problem. We use 200 optimization iterations for each of these choices and then use a fresh batch of 500 samples for each step in the range to calculate final ELBO values. The step with highest final ELBO is selected as the adapted step-size; with the adapted η we optimize for 30,000 iterations where, at each iteration we use 100 total $\log p$ evaluation(same as our other experiments).

We also implement the relative-tolerance convergence criterion implemented in PyStan to detect early convergence(we use a tolerance of 0.001). Also, following the original work, we use the closed form of entropy of q_ϕ for the ADVI training objective. We make an honest attempt to the best of our abilities to re-implement the ADVI and in our preliminary experiments found that the performance matched the PyStan version for the same hyper-parameter settings. We found that the performance of ADVI was highly variable; out of the three independent trials, 9 models diverged in at least one trial. Replacing ADVI step-scheme with our comprehensive step-search saw no divergence for the closed-form entropy case that uses Adam optimizer.

F Implementation details for real-NVP

Architectural details: We use a real-NVP flow with 10 coupling layers for all our experiments. We define each coupling layer to be comprised of two transitions, where a single transition corresponds to affine transformation of one part of the latent variables. For example, if the input variable for the k^{th} layer is $z^{(k)}$, then first transition is defined as :

$$\begin{aligned} z_{1:d} &= z_{1:d}^{(k)} \\ z_{d+1:D} &= z_{d+1:D}^{(k)} \odot \exp(s_k^a(z_{1:d}^{(k)})) + t_k^a(z_{1:d}^{(k)}) \end{aligned} \quad (12)$$

where, super-script a denotes first transition and sub-script k denotes the k^{th} layer. For the next transition, the $z_{d+1:D}$ part is kept unchanged and $z_{1:d}$ is affine transformed in a similar fashion to obtain the layer output $z^{(k+1)}$ (this time using $s_k^b(z_{d+1:D}^{(k)})$ and $t_k^b(z_{d+1:D}^{(k)})$). This is also referred to as the alternating first half binary mask. Both, scale(s) and translation(t) functions are parameterized by the same fully connected neural network(FNN). More specifically, for first transition in above example, a single FNN takes $z_{1:d}^{(k)}$ as input and outputs both $s_k^a(z_{1:d}^{(k)})$ and $t_k^a(z_{1:d}^{(k)})$. Thus, the skeleton of the FNN, in terms of the size of the layers, is as $[d, H, H, 2(D-d)]$ where, H denotes the size of the two hidden layers ($H=32$ for all our experiments).

The hidden layers of FNN use a leaky rectified linear unit with slope = 0.01, while the output layer uses a hyperbolic tangent for s and remains linear for t .

Parameter Initialization: We initialize the parameters of the neural networks from normal distribution $\mathcal{N}(0, 0.001^2)$. We deliberately make this choice as it corresponds to an approximate standard normal initialization for the overall normalizing flow density. To see this, first note that the output from the initialized neural networks will approximately be 0 vectors. Now, consider the affine transformation of real-NVP: at each iteration, we scale by the exponent of s and offset by t . Thus, the overall effect is an identity transform. As the base-distribution is fixed to a standard normal, this gives as an approximate standard normal initialization.

Number of Parameters: For each transition, assuming $d = D/2$, the parameters of the FNN can be calculated as $\frac{1}{2}DH + H^2 + HD + D + 2H$ where D is the number latent dimensions in the model, and H is the size of the two hidden layers. The first three components in the calculation corresponds

to weight matrix, and the latter two take into account the bias parameters. With T coupling layers, each comprising of 2 transitions, the overall parameter size is given by $2T(\frac{3}{2}DH + H^2 + D + 2H)$. We use $T=10$ and $H=32$, while D depends on the problem.

Scaling to higher dimension models: Real NVP based architectures scale better to higher dimensional problems as compared to Gaussians. The parameters in Gaussian scale as $\mathcal{O}(D^2)$ while they scale linearly $\mathcal{O}(D)$ for real-NVP, if we fix other parameters(T and H). However, for lower dimensional problem the number of parameters for real-NVP is more.

G Selection of Best model

We choose the model that achieves best average-objective, averaged over the entire optimization trace. This is different from, perhaps a more natural, final value based selection rule where one evaluates on a smaller batch of fresh samples; smaller compared to number of samples used for final metric evaluation. We found average objective to be more reliable indicator of the performance in practice. In our preliminary experiments, models selected from the maximum average-objective out-performed the ones selected based on the maximum final value; the comparison was based on the final metric value evaluated using a fresh batch of 10,000 samples.

H General comment on trade-offs

We note that a trade-off exists between the improvement in performance and the computational complexity we are prepared to entertain (with the increase in the availability of computational resource, we believe this will increasingly tilt in favor of performance). Using a comprehensive step-search scheme is often done in parallel. However, we do stress that a trade-off exist between spending a higher fixed computational cost vs manually tuning the performance. Adding Laplace Initialization requires one to solve a maximization problem beforehand (this was often inexpensive in our experiments). Adding normalizing flows increase the complexity in terms of both memory and computational time. Adding Importance Weighting with a fixed ‘‘Oracle budget’’ for querying $\log p$ may seem to be relatively inexpensive while training, however, the posterior inference scales linearly in M . Finally, DReG or STL calculation comes at an additional cost for normalizing flows due to a second pass of T_ϕ^{-1} (see [Section 4.3](#) for details).

I Full list of models

We present the complete list of models used in our analysis [Table 1](#). The descriptions in the table have been manually extracted, see Stan-example model repository [\[32\]](#) for more details.

J Complete Table of results

Table 1: This table presents attributes of all the models from the Stan model library [32, 33] that have been used in this analysis. The attribute are $|z|$ = # of latent dimensions, n = # of data points, and $r = \frac{\text{\# of latent dimensions}}{\text{\# of data points}}$

Id	Model name	$ z $	n	r	Model Description
1	lsat	1006	818	1.2298	One-parameter Rasch model for LSAT student response
2	Mh	388	385	1.0078	Heterogeneity model for closed population size estimation from capture-recapture data with individual effects
3	test_simplex	3	10	0.3000	Simplex estimator
4	endo3	184	626	0.2939	Conditional inference model for case-control study on endometrial cancer
5	gp_predict	265	989	0.2679	Model for predicting out-of-sample observations by fitting hyperparams of a latent variable Gaussian process with exponentiated quadratic kernel and Gaussian likelihood
6	Mth	394	1935	0.2036	Combined model for for closed population size estimation with both, time and individual effects
7	oxford	244	1226	0.1990	A mixture model for the log odds ratio to analyze Oxford childhood cancer data
8	cjs_mnl	22	132	0.1667	CJS model for capture-recapture problem with multinomial likelihood
9	hepatitis	218	1596	0.1366	Normal hierarchical model with measurement error in Hb titre in children post Hepatitis vaccination
10	normal_multi	100	826	0.1211	Basic Multi-variate estimators for normal and student-t distributions
11	hiv_chr	173	1476	0.1172	Multi-level linear model with varying slope and intercept for Zinc diet experiment on HIV positive children
12	electric_1c_chr	116	1248	0.0929	Multi-level linear model with varying intercept and slope for the effect of exposure to television show, The Electric Company
13	electric_1a_chr	112	1248	0.0897	Multi-level linear model with group level factors for the effect of exposure to television show, The Electric Company
14	electric_chr	100	1248	0.0801	Multi-level linear model with varying intercept for the effect of exposure to television show, The Electric Company
15	radon_vary_si_chr	175	4595	0.0381	Multi-level linear model with group level predictors to estimate radon levels.
16	lda	33	1157	0.0285	Latent Dirichlet Allocation
17	radon_redundant_chr	88	4595	0.0192	Multi-level linear model with varying intercept and redundant parameterization and the Choo-Hoffman parametrization
18	naive_bayes	39	4124	0.0095	Naive Bayes classifier
19	mesquite_volume	3	322	0.0093	Linear model with one transformed predictor and log transformation to measure the yield of mesquite bushes
20	cjs_t_t	22	3960	0.0056	CJS model for capture-recapture problem with parameter identifiability
21	irt_multilevel	503	90671	0.0055	Item response theory multi-level logistic model
22	irt	501	90941	0.0055	Item response theory 2-p logistic model
23	congress	4	1029	0.0039	Linear model to predict the 1988 election from 1986 election
24	dogs	3	775	0.0039	Multi-level logistic regression model for behavioral learning experiment on dogs
25	Dynocc	29	7500	0.0039	Dynamic (multi-season) site-occupancy Hidden Markov Model
26	multi_logit	32	9842	0.0033	Multinomial logistic regression
27	electric_one_pred	3	1248	0.0024	Lin. model with one predictor
28	election88	55	104094	0.0005	Multi-level logistic regression model with group level predictors to predict Republican candidate in 1988 elections
29	wells	2	15100	0.0001	Generalized linear model with logit link function and one predictor to predict shift to a safer well in Bangladesh
30	wells_dist	2	15100	0.0001	Generalized linear model with logit link function and one predictor to predict shift to a safer well in Bangladesh

Table 2: This table presents the results for ADVI baseline. ADVI runs with high variability in performance; our ADVI implementation diverges for at least 1 random trial for 10 out of 30 models.

	q_ϕ family	Full-rank Gaussian		
	Step-search scheme	ADVI		
	∇_ϕ	Closed form entropy		
	LI	Not Used		
	IWVI M_{training}	1		
	IWVI M_{sampling}	1		
	Method from Outline	ADVI Baseline		
	Independent Trial	Trial 1	Trial 2	Trial 3
Id	Model Name			
1	lsat	nan	nan	nan
2	Mh	19.9685	19.9831	19.9521
3	test_simplex	-4.4433	-4.4408	-4.4373
4	endo3	-127.2903	-127.3857	-127.2958
5	gp_predict	300.0260	300.1867	300.0258
6	Mth	-152.6560	-152.6696	-152.7633
7	oxford	-4401.0033	nan	-4520.5537
8	cjs_mnl	-452.8369	-452.6761	-452.6022
9	hepatitis	-54.1560	-54.1572	-54.1076
10	normal_multi	-40367.4856	-40365.4223	-40368.5330
11	hiv_chr	nan	-74.3163	nan
12	electric_lc_chr	-287.4185	-292.0925	-286.8471
13	electric_la_chr	-428.0037	-429.2815	-437.4855
14	electric_chr	-514.0052	-557.4496	-513.4389
15	radon_vary_si_chr	-102.4855	-102.4855	-102.5110
16	lda	-344.5263	-344.5982	-344.3087
17	radon_redundant_chr	nan	nan	-299.6408
18	naive_bayes	-3615.4987	-3615.4900	-3615.5445
19	mesquite_volume	12.4846	12.4895	nan
20	cjs_t_t	-452.8026	-452.6712	-452.5898
21	irt_multilevel	nan	nan	nan
22	irt	-15460.1601	-15460.3696	-15460.2664
23	congress	736.2241	nan	738.1187
24	dogs	-298.4544	-298.5008	-298.3045
25	Dynocc	-2126.6232	-2126.5978	-2126.6179
26	multi_logit	-554.9885	-554.6617	-554.7382
27	electric_one_pred	nan	nan	-657.4681
28	election88	-7555.5669	-7561.2245	-7556.6900
29	wells_dist	-2274.6544	nan	-2053.4626
30	wells	nan	-2041.9096	nan

Table 3: This table provides results for method that uses the closed-form entropy gradient with our comprehensive step-search scheme. We further provide *additional* the results by using Laplace Initialization scheme and using IW-sampling at inference time.

	q_ϕ family	Full-rank Gaussian											
	Step-search scheme	Comprehensive step-search											
	∇_ϕ	Closed form entropy											
	LI	Not Used											
	IWVI M_{training}	1										Used	
	IWVI M_{sampling}	1										1	
	Method from Outline	(0)										10	
	Independent Trial	Trial 1	Trial 2	Trial 3	10						10		
	Model Name				Additional	Trial 1	Trial 2	Trial 3	Additional	Trial 1	Trial 2	Trial 3	
Id													
1	lsat	-1560.3229	-1560.2861	-1560.2925	-1558.4440	-1558.3792	-1558.4386	-2666.4087	-2667.7454	-2667.5157	-2621.9313	-2622.5349	-2622.8303
2	Mh	19.5196	19.5469	19.5496	20.4490	20.4554	20.4710	19.0324	19.0649	19.0763	20.2788	20.2878	20.2921
3	test_simplex	-4.4463	-4.4483	-4.4402	-4.3669	-4.3745	-4.3603	-4.4438	-4.4453	-4.4496	-4.3673	-4.3731	-4.3702
4	endo3	-127.5089	-127.5777	-127.5220	-121.1431	-121.4293	-121.2687	-127.5829	-127.6264	-127.5953	-121.3321	-121.2752	-121.4067
5	gp_predict	198.4425	202.6357	197.5704	238.4563	238.6492	235.7607	300.0484	299.9787	300.0156	300.9871	300.9911	301.0216
6	Mth	-153.0663	-153.0603	-153.0812	-152.3153	-152.2698	-152.3311	-153.3603	-153.3579	-153.3422	-152.4340	-152.4214	-152.4212
7	oxford	-4333.4364	-4333.9387	-4333.7062	-4331.4304	-4331.5858	-4331.5967	-4.1115e+37	-5.9831e+44	-4.0048e+42	-1.1556e+05	-3.3595e+05	-62689.8962
8	cjs_mnl	-452.6434	-452.6689	-452.6537	-452.0531	-452.0837	-452.0648	-452.6118	-452.6235	-452.6506	-452.0388	-452.0014	-452.0169
9	hepatitis	-54.6239	-54.6593	-54.6598	-53.4851	-53.4839	-53.5132	-161.6031	-161.7103	-161.4679	-156.3505	-156.4540	-156.2607
10	normal_multi	-74650.2692	-74683.3277	-74649.8184	-73234.4113	-72785.9847	-72816.0867	-16918.5887	-16918.5877	-16918.5881	-16918.5857	-16918.5857	-16918.5862
11	hiv_chr	-74.8046	-74.7951	-74.7993	-73.6099	-73.5665	-73.6207	-74.8014	-74.8173	-74.8080	-73.6571	-73.6500	-73.6638
12	electric_1c_chr	-285.7230	-285.8559	-286.4202	-281.1185	-281.2912	-281.4158	-285.6876	-285.9342	-286.3901	-281.1429	-281.3092	-281.3765
13	electric_1a_chr	-424.5786	-424.5153	-424.4387	-422.3741	-422.2738	-422.1691	-424.5125	-424.4337	-424.5577	-422.3750	-422.2143	-422.3517
14	electric_chr	-512.3681	-512.2423	-512.2471	-511.2007	-511.0951	-511.0922	-512.3493	-512.2394	-512.2689	-511.2062	-511.0864	-511.0979
15	radon_vary_si_chr	-102.8430	-102.8273	-102.8068	-101.9041	-101.8598	-101.8806	-102.8266	-102.8438	-102.8082	-101.8498	-101.8824	-101.8779
16	lda	-344.2642	-344.3194	-344.2521	-342.7178	-342.7799	-342.7485	-344.2697	-344.2932	-344.2646	-342.7635	-342.7396	-342.7490
17	radon_redundant_chr	-223.6925	-225.3442	-221.3751	-218.1183	-217.9346	-217.5981	-223.5919	-467.7711	-467.6689	-218.0208	-461.9628	-461.9314
18	naive_bayes	-3615.4642	-3615.4686	-3615.4654	-3615.1421	-3615.1434	-3615.1403	-3615.3055	-3615.3207	-3615.3055	-3615.1060	-3615.1259	-3615.1006
19	mesquite_volume	12.4224	12.3813	12.3800	12.4977	12.5056	12.4976	12.4851	12.4834	12.4865	12.5077	12.5096	12.5132
20	cjs_t_t	-452.6244	-452.6379	-452.6369	-452.0433	-452.0053	-452.0335	-452.6478	-452.6525	-452.6423	-452.0485	-452.0301	-452.0321
21	irt_multilevel	-14611.3903	-14611.3943	-14611.3818	-14609.1618	-14609.1189	-14609.0938	-14608.9681	-14608.9780	-14608.9549	-14608.1255	-14608.1816	-14608.1382
22	irt	-15427.1794	-15427.2162	-15427.1530	-15424.9416	-15424.9849	-15424.8847	-15424.2319	-15424.2349	-15424.2291	-15423.8601	-15423.8488	-15423.8540
23	congress	738.5902	738.4774	738.4840	738.7764	738.6945	738.7785	738.7884	738.7858	738.7842	738.7941	738.7970	738.7933
24	dogs	-298.3675	-298.2871	-298.3304	-298.2795	-298.2588	-298.2810	-298.2638	-298.2646	-298.2660	-298.2594	-298.2597	-298.2593
25	Dynocc	-2126.6299	-2126.6223	-2126.6431	-2125.8526	-2125.8764	-2125.8708	-2126.5057	-2126.4791	-2126.4745	-2125.8125	-2125.7992	-2125.7765
26	multi_logit	-553.8753	-553.8865	-553.8795	-553.4833	-553.4901	-553.5009	-553.5695	-553.5774	-553.5662	-553.4546	-553.4547	-553.4509
27	electric_one_pred	-641.6253	-641.5721	-641.6571	-641.5684	-641.5582	-641.5811	-641.5624	-641.5667	-641.5647	-641.5572	-641.5598	-641.5574
28	election88	-7534.1590	-7534.0445	-7534.1257	-7533.5235	-7533.4941	-7533.5037	-7533.6499	-7533.6635	-7533.6472	-7533.4165	-7533.4340	-7533.4334
29	wells_dist	-2046.5482	-2046.5790	-2046.5165	-2046.5134	-2046.5195	-2046.5087	-2046.5399	-2046.5277	-2046.5413	-2046.5147	-2046.5119	-2046.5111
30	wells	-2041.9656	-2041.9106	-2041.9605	-2041.9170	-2041.9045	-2041.9130	-2041.9045	-2041.9050	-2041.9042	-2041.9043	-2041.9044	-2041.9040

Table 4: This table provides results for Gaussian VI that uses the “full” entropy gradient from Equation (3) with our comprehensive step-search scheme. We further provide *additional* the results when using Laplace Initialization scheme and using IW-sampling at inference time.

q_ϕ family		Full-rank Gaussian											
Step-search scheme		Comprehensive step-search											
∇_ϕ		Estimated without dropping score function term–full gradient											
LI		Used						Not Used					
IWVI M_{training}		1			10			1			10		
IWVI M_{sampling}		1			10			1			10		
Method from Outline		Additional		Additional		Additional		Additional		Additional		Additional	
Independent Trial		Trial 1		Trial 2		Trial 3		Trial 1		Trial 2		Trial 3	
Model Name		Trial 1		Trial 2		Trial 3		Trial 1		Trial 2		Trial 3	
1	lsat	nan	nan	nan	nan	nan	nan	nan	nan	nan	nan	nan	nan
2	Mh	19.0670	19.1056	19.0700	20.3383	20.3370	20.3582	19.5593	19.5481	19.5473	20.4868	20.5185	20.4844
3	test_simplex	-4.4519	-4.4444	-4.4495	-4.3659	-4.3770	-4.3691	-4.4458	-4.4436	-4.4474	-4.3599	-4.3712	-4.3588
4	endo3	-127.5600	-127.5014	-127.5194	-121.3365	-121.2019	-121.2040	-127.4403	-127.5594	-127.5994	-121.1946	-121.2420	-121.3132
5	gp_predict	300.0274	nan	299.9987	300.9504	nan	300.9560	211.0246	195.5789	204.1682	243.6565	234.2550	241.2274
6	Mth	-153.3398	-153.3258	-153.3389	-152.3910	-152.4162	-152.4159	-153.0968	-153.0545	-153.0452	-152.3186	-152.2779	-152.2451
7	oxford	-4.0948e+35	-8.6339e+39	-1.3128e+36	-1.1727e+05	-1.5272e+05	-1.3957e+05	-4333.4798	-4334.0175	-4333.8457	-4331.4394	-4331.5769	-4331.6134
8	cjs_mnl	-452.6258	-452.6614	-452.6494	-452.0289	-452.0753	-452.0496	-452.6556	-452.6672	-452.6334	-452.0531	-452.0783	-452.0089
9	hepatitis	-161.6162	-161.6264	-161.4694	-156.4100	-156.1979	-156.3142	-54.6590	-54.6527	-54.6491	-53.5409	-53.4952	-53.5208
10	normal_multi	-16918.5889	-16918.5874	-16918.5888	-16918.5869	-16918.5853	-16918.5869	-74666.1985	-74664.2850	-74649.3550	-73263.3554	-72766.8331	-72784.2473
11	hiv_chr	-74.8015	-74.7940	-74.8085	-73.6664	-73.6118	-73.6528	-74.7896	-74.8136	-74.7875	-73.6239	-73.6283	-73.5881
12	electric_lc_chr	-285.7864	-285.8934	-286.3494	-281.2761	-281.3296	-281.4412	-285.7462	-286.0667	-286.4748	-281.1279	-281.4554	-281.4536
13	electric_la_chr	-424.4836	-424.4773	-424.5606	-422.2672	-422.2925	-422.3151	-424.4795	-424.5070	-424.4835	-422.2702	-422.2841	-422.2535
14	electric_chr	-512.3679	-512.2732	-512.2296	-511.2040	-511.1366	-511.0640	-512.3744	-512.2624	-512.2523	-511.1901	-511.1049	-511.1025
15	radon_vary_si_chr	-102.8457	-102.8146	-102.8164	-101.8595	-101.8457	-101.8769	-102.8437	-102.8427	-102.7917	-101.9166	-101.9149	-101.8222
16	lda	-344.2699	-344.2947	-344.2570	-342.7400	-342.7795	-342.7185	-344.3098	-344.3006	-344.2416	-342.7539	-342.7678	-342.7477
17	radon_redundant_chr	-467.9613	-467.9049	-467.7597	-462.4864	-462.3585	-462.1381	-223.6050	-2935.5608	-2948.1397	-218.0029	-1613.4442	-1619.0719
18	naive_bayes	-3615.3271	-3615.3214	-3615.3076	-3615.1290	-3615.1298	-3615.1107	-3615.4633	-3615.4660	-3615.4640	-3615.1420	-3615.1252	-3615.1548
19	mesquite_volume	12.4923	12.4882	12.4795	12.5160	12.5119	12.5073	12.4174	12.3694	12.3828	12.4955	12.5047	12.5044
20	cjs_t_t	-452.6280	-452.6403	-452.6759	-452.0359	-452.0043	-452.0893	-452.6438	-452.6591	-452.6367	-452.0456	-452.0408	-452.0151
21	irt_multilevel	-14608.9643	-14608.9678	-14608.9776	-14608.1555	-14608.1392	-14608.1672	-14611.3798	-14611.3839	-14611.3849	-14609.1356	-14609.0725	-14609.1173
22	irt	-15424.2420	-15424.2385	-15424.2292	-15423.8697	-15423.8673	-15423.8487	-15427.2185	-15427.1877	-15427.1430	-15424.9813	-15424.9345	-15424.9523
23	congress	738.7869	738.7817	738.7882	738.7929	738.7934	738.7973	738.6008	738.4618	738.4788	738.7810	738.6687	738.7758
24	dogs	-298.2633	-298.2652	-298.2677	-298.2589	-298.2598	-298.2612	-298.3626	-298.2907	-298.3202	-298.2743	-298.2622	-298.2661
25	Dynocc	-2126.4982	-2126.4909	-2126.5233	-2125.7935	-2125.7953	-2125.8381	-2126.6111	-2126.6211	-2126.5974	-2125.8136	-2125.8503	-2125.8062
26	multi_logit	-553.5636	-553.5538	-553.5567	-553.4501	-553.4276	-553.4351	-553.8916	-553.8986	-553.8756	-553.4952	-553.5075	-553.4867
27	electric_one_pred	-641.5643	-641.5670	-641.5643	-641.5585	-641.5605	-641.5569	-641.6257	-641.5759	-641.6568	-641.5661	-641.5609	-641.5806
28	election88	-7533.6598	-7533.6606	-7533.6501	-7533.4296	-7533.4350	-7533.4345	-7534.1616	-7534.0692	-7534.1277	-7533.5377	-7533.5224	-7533.5308
29	wells_dist	-2046.5415	-2046.5281	-2046.5470	-2046.5172	-2046.5110	-2046.5149	-2046.5478	-2046.5839	-2046.5186	-2046.5136	-2046.5238	-2046.5112
30	wells	-2041.9040	-2041.9044	-2041.9042	-2041.9038	-2041.9038	-2041.9040	-2041.9630	-2041.9106	-2041.9583	-2041.9132	-2041.9043	-2041.9110

Table 5: This table provides results when using STL gradient from Equation (3) with our comprehensive step-search scheme. We further provide *additional* the results when using Laplace Initialization scheme and using IW-sampling at inference time.

Id	q_ϕ family Step-search scheme ∇_ϕ LI IWVI M_{training} IWVI M_{sampling} Method from Outline Independent Trial Model Name	Full-rank Gaussian Comprehensive step-search Estimate with STL Used						Not Used			10 (3a)		
		10 Additional						1 (1)					
		Trial 1	Trial 2	Trial 3	Trial 1	Trial 2	Trial 3	Trial 1	Trial 2	Trial 3	Trial 1	Trial 2	Trial 3
1	lsat	-4091.5673	-4091.2330	-4092.0852	-4056.4919	-4056.1063	-4055.9834	-1558.7810	-1558.7472	-1558.7390	-1557.7991	-1557.7429	-1557.7450
2	Mh	20.0356	20.0303	20.0047	20.6543	20.6089	20.6071	20.0312	20.0099	20.0382	20.6310	20.5794	20.6332
3	test_simplex	-4.4462	-4.4426	-4.4465	-4.3756	-4.3697	-4.3621	-4.4479	-4.4497	-4.4429	-4.3757	-4.3774	-4.3707
4	endo3	-127.4334	-127.4200	-127.4744	-121.3711	-121.3008	-121.3031	-127.4760	-127.4425	-127.3645	-121.2750	-121.3448	-121.1234
5	gp_predict	300.3652	300.3384	300.3369	301.0796	301.0768	301.0742	221.0104	184.9239	199.2730	251.7177	229.4787	236.0091
6	Mth	-152.5692	-152.5807	-152.5665	-152.1654	-152.1577	-152.1657	-152.5853	-152.5776	-152.5712	-152.1531	-152.1763	-152.1694
7	oxford	-4.7437e+37	-1.6905e+39	-6.5444e+38	-1.0902e+05	-63518.2033	-2.0817e+05	-4332.4161	-4332.8902	-4332.2031	-4331.2022	-4331.2105	-4331.0641
8	cjs_mnl	-452.5887	-452.6104	-452.6059	-452.0214	-452.0512	-452.0276	-452.5971	-452.6071	-452.5779	-452.0397	-452.0621	-452.0186
9	hepatitis	-158.9974	-159.0309	-159.2058	-154.5824	-154.7220	-154.8867	-53.7993	-53.8159	-53.8126	-53.1213	-53.1084	-53.0708
10	normal_multi	-16918.5862	-16918.5866	-16918.5863	-16918.5861	-16918.5860	-16918.5862	-74671.5739	-74669.7508	-74673.7012	-73242.5592	-72773.3522	-72815.9822
11	hiv_chr	-74.2120	-160.9142	-160.7770	-73.4592	-153.4229	-153.1253	-74.1980	-74.2091	-74.2213	-73.4454	-73.4351	-73.4323
12	electric_1c_chr	-284.9183	-285.3767	-284.2679	-280.8849	-280.9905	-280.4814	-284.8103	-285.3329	-284.1304	-280.8633	-280.9278	-280.5198
13	electric_1a_chr	-423.6188	-423.5255	-423.5899	-421.9740	-421.9125	-421.8940	-423.6309	-423.5165	-423.6198	-421.9503	-421.9002	-421.9364
14	electric_chr	-511.5287	-511.4958	-511.6702	-510.9102	-510.9387	-510.9712	-511.5600	-511.5064	-511.6432	-510.9402	-510.9655	-510.9761
15	radon_vary_si_chr	-211.7987	-212.1275	-212.0410	-204.6177	-204.6255	-204.6489	-102.3823	-102.3710	-102.3839	-101.7380	-101.6922	-101.7524
16	lda	-344.2253	-344.2154	-344.2544	-342.7557	-342.7557	-342.7813	-344.2538	-344.2386	-344.2659	-342.7780	-342.7440	-342.8067
17	radon_redundant_chr	-467.5724	-557.4908	-466.8820	-463.1025	-532.0482	-462.2899	-2924.6354	-2934.9166	-2954.9253	-1563.8479	-1611.5559	-1629.3424
18	naive_bayes	-3615.2914	-3615.2818	-3615.2835	-3615.1175	-3615.1048	-3615.1145	-3615.2889	-3615.2737	-3615.2853	-3615.1151	-3615.1053	-3615.1192
19	mesquite_volume	12.4858	12.4884	12.4881	12.5083	12.5136	12.5123	12.4874	12.4614	12.4514	12.5127	12.5060	12.5069
20	cjs_t_t	-452.5757	-452.5689	-452.6060	-451.9996	-452.0086	-452.0482	-452.5950	-452.5798	-452.5913	-452.0293	-452.0230	-452.0237
21	irt_multilevel	-14608.3948	-14608.3807	-14608.3959	-14608.0374	-14608.0328	-14608.0398	-14608.3791	-14608.3849	-14608.3966	-14608.0311	-14608.0351	-14608.0415
22	irt	-15424.0709	-15424.1942	-15424.0688	-15423.8320	-15423.8400	-15423.8318	-15424.1996	-15424.2093	-15424.2063	-15423.8217	-15423.8582	-15423.8520
23	congress	738.7871	738.7906	738.7895	738.7920	738.7954	738.7949	738.7803	738.7863	738.7861	738.7929	738.7949	738.7942
24	dogs	-298.2638	-298.2635	-298.2641	-298.2591	-298.2595	-298.2590	-298.2680	-298.2696	-298.2644	-298.2587	-298.2580	-298.2577
25	Dynocc	-2126.5165	-2126.5050	-2126.4933	-2125.7914	-2125.8100	-2125.7789	-2126.5121	-2126.5112	-2126.4865	-2125.8071	-2125.8183	-2125.7419
26	multi_logit	-553.5765	-553.5475	-553.5493	-553.4467	-553.4340	-553.4499	-553.5746	-553.5669	-553.5647	-553.4531	-553.4447	-553.4312
27	electric_one_pred	-641.5628	-641.5642	-641.5635	-641.5576	-641.5578	-641.5579	-641.5701	-641.5706	-641.5667	-641.5591	-641.5604	-641.5600
28	election88	-7533.5352	-7533.5890	-7533.5733	-7533.3942	-7533.4317	-7533.4243	-7533.5530	-7533.5750	-7533.5676	-7533.4176	-7533.4129	-7533.4223
29	wells_dist	-2046.5099	-2046.5101	-2046.5099	-2046.5090	-2046.5090	-2046.5090	-2046.5104	-2046.5095	-2046.5094	-2046.5098	-2046.5093	-2046.5092
30	wells	-2041.9040	-2041.9040	-2041.9040	-2041.9039	-2041.9039	-2041.9040	-2041.9041	-2041.9039	-2041.9041	-2041.9040	-2041.9037	-2041.9040

Table 6: This table provides results for importance-weighted training for Gaussian q_ϕ optimized with our comprehensive step-search scheme. We further provide *additional* the results when using Laplace Initialization scheme and using the regular IW-ELBO gradient of Equation (5)

Id	q_ϕ family	Full-rank Gaussian			Estimated with DReG			Not Used			Not Used		
	Step-search scheme	Comprehensive step-search			Estimated without dropping the score-function term			Used			Used		
	∇_ϕ	Used			Not Used			Used			Not Used		
	LI	10			10			10			10		
	IWVI M_{training}	10			10			10			10		
	IWVI M_{sampling}	10			10			10			10		
	Method from Outline	Additional			Additional			Additional			(3b)		
	Independent Trial	Trial 1			Trial 1			Trial 1			Trial 1		
	Model Name	Trial 2			Trial 2			Trial 2			Trial 2		
		Trial 3			Trial 3			Trial 3			Trial 3		
1	lsat	nan	nan	nan	nan	nan	nan	-3602.4668	-3626.9508	-3561.9721	-1560.4725	-1560.6102	-1560.2753
2	Mh	15.4818	15.7472	15.6913	19.7892	19.7846	19.8196	19.3155	19.1917	19.1727	20.7624	20.7138	20.7093
3	test_simplex	-4.3528	-4.3557	-4.3442	-4.3538	-4.3437	-4.3491	-4.3460	-4.3477	-4.3570	-4.3503	-4.3525	-4.3501
4	endo3	-121.0991	-121.1391	-121.1125	-120.9746	-121.1293	-121.0337	-120.6768	-120.6442	-120.7764	-120.7299	-120.6274	-120.7329
5	gp_predict	nan	300.6958	300.6468	300.7821	300.8882	300.7675	301.4711	301.4523	301.4776	301.5145	301.4983	nan
6	Mth	-157.6131	-157.8043	-157.8328	-152.9738	-152.8934	-152.9296	-154.0925	-154.0752	-153.8830	-152.0879	-152.0961	-152.0757
7	oxford	-1.9933e+05	-5.0506e+05	-74206.7353	-4345.0453	-4347.0228	-4346.2444	-4.9035e+05	-1.2894e+05	-37340.6443	-4344.8534	-4343.0004	-4343.6250
8	cjs_mnl	-451.8801	-451.8757	-451.8600	-451.9819	-451.9677	-451.9664	-451.8670	-451.8624	-451.8923	-451.8809	-451.8810	-451.8503
9	hepatitis	-169.5314	-170.4767	-169.9543	-69.2357	-69.3825	-70.9711	-168.6359	-168.2180	-168.8426	-55.9312	-56.1853	-56.6067
10	normal_multi	-16918.5870	-16918.5937	-16918.5867	-26750.2857	-27498.9976	-27460.3790	-16918.5864	-16918.5864	-16918.5863	-27788.4873	-26875.6551	-27865.8058
11	hiv_chr	-176.5920	-175.6895	-171.8587	-74.9593	-74.9456	-75.1526	-174.1049	-170.4290	-170.1433	-73.5738	-73.5807	-73.6530
12	electric_1c_chr	-286.7872	-287.3433	-286.7932	-315.0138	-313.2617	-315.6589	-285.7240	-286.3400	-284.3945	-310.0764	-314.5847	-311.5810
13	electric_1a_chr	-426.9384	-426.9405	-428.7423	-426.9211	-428.3849	-428.2209	-422.5884	-426.4747	-430.4513	-422.5316	-422.7934	-423.0203
14	electric_chr	-516.2415	-516.4791	-516.0333	-516.2482	-516.6440	-515.8745	-515.7389	-515.3542	-514.7078	-515.9188	-515.7946	-515.8023
15	radon_vary_si_chr	-103.8548	-104.1821	-103.7281	-102.8569	-102.9285	-102.9329	-178.6936	-181.2776	-175.7665	-101.6374	-101.6283	-101.6344
16	lda	-342.3627	-342.3805	-342.3895	-342.4098	-342.3976	-342.4005	-342.3420	-342.3486	-342.2886	-342.3074	-342.3318	-342.3201
17	radon_redundant_chr	-356.7974	-453.5837	-358.3671	-693.8210	-693.9595	-3186.8453	-449.6303	-449.8883	-452.8245	-671.9259	-691.9953	-3202.9959
18	naive_bayes	-3615.0965	-3615.1078	-3615.0916	-3615.3434	-3615.3476	-3615.3793	-3615.0964	-3615.1020	-3615.1063	-3615.1163	-3615.0989	-3615.0960
19	mesquite_volume	12.5129	12.5125	12.5134	12.3802	12.3888	12.2544	12.5120	12.5108	12.5123	12.5071	12.5101	12.5141
20	cjs_t_t	-451.8701	-451.8341	-451.8730	-452.0175	-451.9672	-452.0109	-451.9038	-451.8530	-451.8859	-451.8573	-451.8625	-451.8934
21	irt_multilevel	-14609.2097	-14609.3464	-14608.4966	-14622.5119	-14622.2421	-14622.6026	-14607.9892	-14608.0042	-14608.0028	-14611.7850	-14611.8132	-14611.5983
22	irt	-15423.9092	-15423.9159	-15423.9325	-15437.7767	-15437.2800	-15437.1353	-15423.8471	-15423.8396	-15423.8208	-15424.2517	-15423.9661	-15427.9253
23	congress	738.7864	738.7833	738.7801	738.6621	738.5947	738.6958	738.7922	738.7937	738.7952	738.7948	738.7948	738.7956
24	dogs	-298.2718	-298.2617	-298.2698	-298.4308	-298.4959	-298.3189	-298.2585	-298.2587	-298.2598	-298.2605	-298.2574	-298.2614
25	Dynocc	-2125.6550	-2125.6638	-2125.7156	-2125.8873	-2125.9113	-2125.8858	-2125.6986	-2125.6466	-2125.5890	-2125.6676	-2125.6854	-2125.6376
26	multi_logit	-553.5210	-553.5132	-553.4919	-554.1409	-553.8148	-554.0896	-553.4295	-553.4241	-553.4322	-553.4322	-553.4350	-553.4397
27	electric_one_pred	-641.5591	-641.5585	-641.5581	-641.9277	-641.7308	-641.6937	-641.5579	-641.5594	-641.5546	-641.5589	-641.5605	-641.5588
28	election88	-7533.4531	-7533.4451	-7533.4654	-7534.4716	-7534.6690	-7534.5011	-7533.4137	-7533.4106	-7533.4142	-7533.4076	-7533.4078	-7533.4052
29	wells_dist	-2046.5308	-2046.5357	-2046.5255	-2046.6939	-2046.5931	-2046.5876	-2046.5091	-2046.5093	-2046.5089	-2046.5092	-2046.5090	-2046.5089
30	wells	-2041.9053	-2041.9222	-2041.9059	-2042.0735	-2041.9343	-2042.0528	-2041.9041	-2041.9040	-2041.9039	-2041.9040	-2041.9039	-2041.9039

Table 7: This table provides results for real-NVP normalizing flows optimized with our comprehensive step-search scheme with additional results from using IW-sampling.

q_ϕ family		Real NVP flows											
Step-search scheme		Comprehensive step-search						Estimated with STL					
∇_ϕ		Estimated without dropping the score-function term–full gradient						Not Used					
LI		Not Used						Not Used					
IWVI M _{training}		1						1					
IWVI M _{sampling}		1						1					
Method from Outline		10						10					
Independent Trial		(4a)		Additional		(4b)		(4c)					
Model Name		Trial 1	Trial 2	Trial 3	Trial 1	Trial 2	Trial 3	Trial 1	Trial 2	Trial 3	Trial 1	Trial 2	Trial 3
1	lsat	-1558.0810	-1558.0983	-1558.0795	-1557.4331	-1557.4355	-1557.4532	-1557.7891	-1557.7745	-1557.7618	-1557.3710	-1557.3581	-1557.3378
2	Mh	20.6116	20.6099	20.5906	21.0692	21.0748	21.0498	20.8141	20.7952	20.7906	21.1431	21.1399	21.1405
3	test_simplex	nan	nan	nan	nan	nan	nan	nan	nan	nan	nan	nan	nan
4	endo3	-125.4364	-125.6489	-125.3696	-119.9958	-120.1006	-119.8449	-124.1439	-124.6179	-123.8879	-119.0637	-119.4145	-118.8396
5	gp_predict	301.0234	300.9385	133.3838	301.8497	301.8672	175.2945	291.8903	186.8792	278.3282	295.9186	222.9463	287.6078
6	Mth	-152.0877	-152.1042	-152.0981	-151.8264	-151.8418	-151.8434	-151.9116	-151.8974	-151.9065	-151.7999	-151.7864	-151.7871
7	oxford	-4332.3919	-4332.4422	-4332.3601	-4331.2495	-4331.2409	-4331.2086	-4331.7142	-4331.7552	-4331.6724	-4330.9652	-4330.9303	-4330.9149
8	cjs_mnl	-451.6828	-451.6553	-451.7014	-451.5297	-451.5138	-451.5268	-451.5370	-451.5515	-451.5312	-451.5047	-451.5007	-451.5000
9	hepatitis	-52.1719	-52.0280	-51.9546	-51.3164	-51.2786	-51.1834	-51.1649	-51.1504	-51.0317	-50.8315	-50.7965	-50.7713
10	normal_multi	-16937.4055	-16924.0775	-16940.7436	-16930.1828	-16920.9157	-16930.9541	-16919.3660	-16933.2347	-16919.2307	-16918.7303	-16926.7185	-16918.7138
11	hiv_chr	-74.0555	-74.4123	-74.2517	-73.0828	-73.2133	-73.1843	-73.1723	-73.0908	-73.1615	-72.8201	-72.7956	-72.8215
12	electric_1c_chr	-279.5105	-279.2506	-278.9096	-278.1362	-278.0216	-277.9078	-278.1784	-278.8128	-278.2789	-277.6591	-277.8439	-277.6683
13	electric_1a_chr	-420.8645	-420.9422	-420.8577	-420.2430	-420.2319	-420.2248	-420.2447	-420.3372	-420.2873	-420.0749	-420.1021	-420.0974
14	electric_chr	-510.9007	-510.8399	-511.0042	-510.6317	-510.6201	-510.6661	-510.6236	-510.6386	-510.6629	-510.6001	-510.6022	-510.6002
15	radon_vary_si_chr	-102.3573	-102.2121	-102.0270	-101.5372	-101.5044	-101.4406	-101.4443	-101.5437	-101.4984	-101.3241	-101.3366	-101.3272
16	lda	nan	-343.8487	nan	nan	-342.5254	nan	nan	nan	nan	nan	nan	nan
17	radon_redundant_chr	-217.3711	-217.2081	-217.2531	-216.9475	-216.9049	-216.9103	-216.9012	-217.0216	-216.9071	-216.8625	-216.8828	-216.8627
18	naive_bayes	-3615.3514	-3615.2491	-3615.3346	-3615.1268	-3615.1000	-3615.1178	-3615.0951	-3615.1031	-3615.1061	-3615.0718	-3615.0772	-3615.0768
19	mesquite_volume	12.4818	12.4943	12.4949	12.5128	12.5150	12.5175	12.5073	12.4761	12.5053	12.5132	12.5085	12.5139
20	cjs_t_t	-451.6751	-451.6590	-451.6910	-451.5173	-451.5230	-451.5276	-451.5337	-451.5676	-451.5380	-451.5010	-451.5019	-451.5029
21	irt_multilevel	-14609.0529	-14609.1944	-14609.0893	-14608.1901	-14608.2447	-14608.2274	-14608.3838	-14608.3419	-14608.3424	-14608.0398	-14608.0113	-14608.0313
22	irt	-15425.1807	-15425.0129	-15424.9788	-15424.1654	-15424.0792	-15424.0399	-15424.3563	-15424.2689	-15424.2745	-15423.8821	-15423.8861	-15423.8640
23	congress	738.7674	738.6810	738.4917	738.7953	738.7737	738.7619	738.6337	738.7920	738.5114	738.7762	738.7957	738.7648
24	dogs	-298.3447	-303.0714	-298.2653	-298.2672	-302.1189	-298.2595	-298.2593	-298.2587	-298.2587	-298.2587	-298.2580	-298.2578
25	Dynocc	-2125.4343	-2125.4809	-2125.4959	-2125.1858	-2125.2057	-2125.2117	-2125.2266	-2125.2430	-2125.2304	-2125.1621	-2125.1556	-2125.1584
26	multi_logit	-554.3855	-554.2881	-554.4112	-553.6644	-553.6392	-553.6909	-553.8005	-553.8478	-553.8052	-553.4846	-553.5251	-553.4879
27	electric_one_pred	-641.6955	-641.5924	-641.7577	-641.5716	-641.5595	-641.5836	-641.5577	-641.5823	-641.5729	-641.5568	-641.5594	-641.5580
28	election88	-7533.5399	-7533.5842	-7533.6034	-7533.4097	-7533.4182	-7533.4205	-7533.4139	-7533.3991	-7533.4044	-7533.3948	-7533.3908	-7533.3919
29	wells_dist	-14358.7734	-2053.1972	-2066.2398	-2107.7104	-2052.5297	-2052.9980	-2046.5242	-2046.5117	-2046.5132	-2046.5109	-2046.5098	-2046.5107
30	wells	-2053.2450	-2128.8088	-2043.5417	-2052.6375	-2057.4116	-2043.0341	-2041.9040	-2041.9045	-2041.9038	-2041.9039	-2041.9043	-2041.9037

Table 8: This table provides results for importance weighted training for real-NVP normalizing flows optimized with our comprehensive step-search scheme with additional results from using regular IW-ELBO gradient.

Id	q_ϕ family	Real NVP flows					
	Step-search scheme	Comprehensive step-search			Estimated with DReG		
	∇_ϕ	Estimated w/o dropping score-function term			Not Used		
	LI	Not Used			Not Used		
	IWVI M_{training}	10			10		
	IWVI M_{sampling}	10			10		
	Method from Outline	Additional			(4d)		
	Independent Trial	Trial 1			Trial 1		
	Model Name	Trial 2			Trial 2		
		Trial 3			Trial 3		
1	lsat	-1557.7324	-1557.7093	-1557.7707	-1557.3724	-1557.3555	-1557.3413
2	Mh	20.8262	20.8106	20.8031	21.1380	21.1331	21.1265
3	test_simplex	nan	nan	nan	nan	nan	nan
4	endo3	-120.3320	-120.4250	-120.4874	-120.0272	-119.9676	-120.1827
5	gp_predict	300.1498	300.0910	300.6795	301.7336	301.7699	301.7164
6	Mth	-151.9868	-152.0086	-152.0120	-151.8052	-151.7779	-151.8100
7	oxford	-4332.1323	-4332.3033	-4332.4134	-4331.0128	-4331.0230	-4330.9522
8	cjs_mnl	-451.7348	-451.7418	-451.7667	-451.5060	-451.5204	-451.5041
9	hepatitis	-52.2705	-52.4800	-52.5429	-50.8712	-51.2069	-50.8934
10	normal_multi	-16933.1393	-16940.4390	-16935.3070	-16920.0900	-16922.8421	-16937.6249
11	hiv_chr	-74.9543	-75.1996	-75.2645	-73.0401	-72.9434	-72.8453
12	electric_1c_chr	-279.7025	-279.6760	-279.8671	-278.0520	-278.2926	-278.3740
13	electric_1a_chr	-421.0590	-421.0157	-421.1706	-420.1473	-420.1479	-420.1098
14	electric_chr	-510.8465	-511.4763	-510.9585	-510.6169	-510.6045	-510.6419
15	radon_vary_si_chr	-102.8107	-102.1768	-102.3642	-101.6430	-101.3792	-101.3284
16	lda	-342.2148	-342.1463	-341.9619	-342.1034	nan	-342.1726
17	radon_redundant_chr	-217.5033	-217.3719	-217.3199	-219.1729	-216.8761	-216.8774
18	naive_bayes	-3615.2138	-3615.1675	-3615.2120	-3615.0806	-3615.0806	-3615.0849
19	mesquite_volume	12.4558	12.4775	12.4488	12.4897	12.5151	12.5162
20	cjs_t_t	-451.6491	-451.6962	-451.7152	-451.7311	-451.5933	-451.5014
21	irt_multilevel	-14609.2872	-14609.3237	-14609.3317	-14608.0970	-14608.0508	-14608.0362
22	irt	-15424.9266	-15425.1680	-15424.9245	-15423.8881	-15423.9093	-15423.9310
23	congress	738.7386	738.7660	738.7162	738.7869	738.7954	738.7907
24	dogs	-298.3505	-298.2761	-298.2739	-298.2580	-298.2586	-298.2581
25	Dynocc	-2125.3477	-2125.3606	-2125.3213	-2125.1688	-2125.1674	-2125.1792
26	multi_logit	-555.2918	-556.6276	-555.3734	-556.2806	-553.5680	-554.7593
27	electric_one_pred	-641.6248	-641.5941	-641.6119	-641.5573	-641.5567	-641.5628
28	election88	-7533.5460	-7533.6522	-7533.6817	-7533.3927	-7533.4052	-7533.3914
29	wells_dist	-2046.7589	-2057.7702	-2046.6208	-2046.5093	-2046.5150	-2046.5097
30	wells	-2047.6023	-2041.9124	-2041.9151	-2041.9042	-2041.9042	-2041.9038